Research Article

Comparison of Human Recombinant Protein Coatings and Fibroblast-ECM to Matrigel for Induced Pluripotent Stem Cell Culture and Renal Podocyte Differentiation

Cormac Murphy[1], Elisabeth Naderlinger[1], Amber Mater[1], Roelof J. C. Kluin[2] and Anja Wilmes[1]

[1]Division of Molecular and Computational Toxicology, Department of Chemistry and Pharmaceutical Sciences, Vrije Universiteit Amsterdam, Amsterdam, The Netherlands; [2]Genomics core facility, Netherlands Cancer Institute (NKI), Amsterdam, The Netherlands

Abstract

Human induced pluripotent stem cells (hiPSCs) offer great opportunities within the 3R framework. In the field of toxicology, they may contribute greatly to the reduction and eventually replacement of animal models. However, culturing hiPSCs as well as differentiation of hiPSCs into target cells that are used for toxicity testing depend on the presence of extracellular matrix (ECM) coating the growth surface. The most widely used ECM is Matrigel®, an animal product that is derived from mouse sarcoma. Drawbacks of Matrigel are widely recognized and include batch-to batch variations, use of animal rather than human material, and ethical concerns about its production. While alternative coatings exist, higher cost and limited characterizations may hinder their broader uptake by the scientific community. Here, we report an extensive comparison of three commercially available human ECM coatings, vitronectin, laminin-511, and laminin-521, to Matrigel in three different hiPSC lines in long-term culture (≥ 9 passages). Characterization included expression of pluripotent markers in a genome-wide transcriptomics study (TempO-Seq), capacity to differentiate into embryoid bodies, and karyotype stability assessed by analyzing copy number variations by shallow DNA sequencing. Furthermore, a low-cost, decellularized ECM produced by human neonatal dermal fibroblasts was tested. In addition, all alternative coatings were tested for hiPSC differentiation into renal podocyte-like cells in a genome-wide transcriptomics screen. Our results show that all tested coatings were highly comparable to animal-derived Matrigel for both hiPSC maintenance and differentiation into renal podocyte-like cells. Furthermore, decellularized fibroblast-ECM could be a novel, attractive low-cost coating material.

1 Introduction

Since the discovery of induced pluripotent stem cells (iPSCs) (Takahashi and Yamanaka, 2006), their potential in regenerative medicine and toxicity testing has been widely recognized (Inoue et al., 2014). The possibility to use iPSCs from various donors, both healthy individuals and patients carrying genetic diseases, allows to better represent the human population on the one hand and to capture and understand personalized responses on the other hand. In terms of replacement of animal use in scientific experiments, human iPSCs (hiPSCs) are discussed as a potential gamechanger in efficacy and adverse effect screening (Suter-Dick et al., 2015). However, it is not well recognized that the most widely used coating for iPSC growth surfaces under feeder-cell free conditions, Matrigel® (or equivalent products licensed under different names, e.g., Geltrex™), is derived from animals.

In vivo, cells are surrounded and embedded in an extracellular matrix (ECM), a network of proteins and polysaccharides that provide not only the structure for cell attachment but also regulate processes in cell homeostasis and communication (signal transduction) among the cells (Frantz et al., 2010; Theocharis et al., 2016). While many cells cultured *in vitro* produce their own ECM, the culture of iPSCs requires culture dishes to be coated with ECM proteins for cell attachment. The most commonly used coating for iPSC culture, Matrigel, is produced by isolating Engelbreth-Holm-Swarm (EHS) sarcomas in mice (Kibbey, 1994). Its production raises not only concerns of batch-to-batch variations, but also major ethical concerns, as mice are injected with

Received December 20, 2021; Accepted June 1, 2022;
Epub June 20, 2022; © The Authors, 2023.

ALTEX 40(1), 141-159. doi:10.14573/altex.2112204

Correspondence: Anja Wilmes, Assistant Professor, PhD
Division of Molecular and Computational Toxicology
Vrije Universiteit Amsterdam
De Boelelaan 1108
1081HZ Amsterdam, The Netherlands
(a.wilmes@vu.nl)

the tumor and sacrificed for the harvesting after it has grown. In the protocol described by Kibbey (1994), 20-25 mice are required to harvest 100 g tumor material (sufficient for producing 1 L Matrigel at a concentration of 10 to 15 mg/mL). With an average weight of 20-25 g per mouse and a tumor weight of 4-5 g per animal, the tumor accounts for up to 20% of the mouse's total body weight when it is harvested.

While alternative coatings, including vitronectin and various laminins are commercially available, these are not as widely used by the scientific community as Matrigel. Reasons for this may include concerns about their long-term effects on karyotype stability (Liu et al., 2014; Kang et al., 2015) as well as limited comparison studies that often do not include multiple iPSC lines or were only tested over few passage numbers. In addition, comparison of these studies is challenging due to differences in culture conditions, including use of different culture media. Moreover, the often much higher price of recombinant proteins in comparison to Matrigel may be an issue.

One of the more widely used alternative recombinant protein coatings for the maintenance of hiPSCs is the glycoprotein vitronectin that was first described in human serum in 1967 by Holmes and later identified to be present in tissue (Holmes, 1967; Hayman et al., 1983). Vitronectin contains a tripeptide arginine-glycine-aspartic acid (RGD) site (Suzuki et al., 1985) that binds to integrins, which are in turn involved in the attachment of cells to the ECM (Meredith et al., 1996). A truncated version of the human recombinant protein (VTN-N) has been shown to be suitable for hiPSC culture in E8 medium (Chen et al., 2011). However, comparison studies to Matrigel, under identical conditions, are sparse. While one study concluded that colony growth was slower and pluripotent markers were less expressed in hiPSCs cultured on vitronectin in E8 medium compared to hiPSCs cultured on Matrigel in mTeSR™1 medium (Hey et al., 2018), it is unclear whether these differences were due to the different coating or the different media. One study reports that recombinant vitronectin was comparable to Matrigel for culturing human embryonic stem cells (hESCs) (Braam et al., 2008) and a single hiPSC cell line (Rowland et al., 2010).

Other recombinant human proteins tested for hiPSC maintenance include the glycoproteins fibronectin and various laminins. One study reported hiPSC attachment and proliferation on laminin and fibronectin using mTeSR™1 medium, but also found lower gene expression of the pluripotency markers *POU5F1* (aka *Oct3/4*), *NANOG*, and *KLF4* compared to hiPSCs grown on Matrigel (Lam and Longaker, 2012). However, it did not state which of the more than sixteen subtypes of laminin was used in the study (Burgeson et al., 1994). Rodin et al. (2014) suggested that hESCs express the 4 laminin subtypes laminin-511, laminin-521, laminin-111 and laminin-121 and studied the survival of hESCs on these recombinant protein coatings, showing that laminin-511 and laminin-521 achieved the best cell attachment and survival after 24 h. The laminin subtypes 511 and 521 have been proposed to be suitable for pluripotent stem cell culture in other studies as well. Laminin-511 was evaluated in hESCs and hiPSCs (Rodin et al., 2010), laminin-521 was evaluated using hESCs (Albalushi et al., 2018) and hiPSCs (Lu et al., 2014), and a combination of laminin-521 and E-cadherin was tested in hESCs and hiPSCs (Rodin et al., 2014). However, different experimental settings among these studies, including different culture media (KO-DMEM, O3, E8, NutriStem™ TeSR™2 and mTeSR™1), again make it difficult to directly compare these among each other or to the widely used Matrigel in mTeSR™1 medium.

The aim of this study was to directly compare the alternative commercial coatings vitronectin, laminin-511, and laminin-521 as well as a low-cost in-house produced ECM derived from human neonatal foreskin fibroblasts to animal-derived Matrigel using three different hiPSC lines cultured under identical culture settings. We evaluated pluripotent markers via high-content imaging (HCI) and differentiation into embryoid bodies (EBs) as well as parameters that had not previously been reported for alternative coatings in hiPSCs, including copy number variations (CNVs) and full genome transcriptomics (TempO-Seq). Differentiation of hiPSCs into renal podocytes (Rauch et al., 2018) was performed on all alternative coatings and compared to podocyte differentiation on Matrigel by analyzing podocyte markers via HCI and full-genome TempO-Seq transcriptomics.

2 Material and methods

iPSC culture

The human iPSC lines SFC086 (clone 1), SBAD3 (clone 1), and SBAD2 (clone 1) were obtained from the IMI StemBANCC project (Morrison et al., 2015). iPSCs were reprogrammed using Sendai virus (Cytotune 2.0) as previously described (Chichagova et al., 2016). Short tandem repeat (STR) profiles are reported in Table S1[1]. These cell lines were routinely cultured in mTeSR™1 (StemCell Technologies, cat. 85850) on Geltrex™ (8 µg/cm^2) (Gibco, cat. A1413302) coated plates at 36.5°C in 5% CO_2 as previously described (Murphy et al., 2019). iPSCs were sub-cultured twice a week using 0.02% Versene® (EDTA, Lonza, cat. BE17-711E) and splitting ratios between 1:3 and 1:10. All cells tested negative for mycoplasma contaminations using the MycoAlert Mycoplasma Detection Kit (Lonza, cat. LT07-318). Cells were inspected visually and by phase-contrast microscopy to rule out bacterial and fungal contaminations. Prior to switching cells to commercial alternative coatings, the following passage numbers (P) of the three cell lines were recorded: P34 (SBAD2), P36 (SBAD3), and P20 (SFC086).

Alternative commercial coatings were prepared in sterile Dulbecco's phosphate buffered saline without magnesium and calcium (DPBS) (Gibco, cat. 141900169) according to the manufacturers' instructions. In short, ECMatrix™-511 (laminin-511) (Merck Millipore, cat. CC160-1050UG) was diluted to a final concentration of 0.25 µg/cm^2, recombinant human laminin-521 (Gibco, cat. A29248) was diluted to a final concentration of 0.5 µg/cm^2, and

[1] doi:10.14573/altex.2112204s1

truncated recombinant human vitronectin (VTN-N) (Gibco, cat. A14700) was diluted to a final concentration of 0.5 µg/cm^2.

Harvesting of ECM from decellularized human foreskin fibroblasts

Human foreskin fibroblasts fHDF/TERT166 immortalized with hTERT were obtained from Evercyte GmbH, Vienna, Austria. STR profiles are shown in Table S1[1]. Cells were routinely cultured in DMEM (Gibco, cat. 11966-025) and Ham's F12 Nutrient Mix (Gibco, cat. 21765-029) (1:1), enriched with penicillin-streptomycin (100 U/mL and 100 µg/mL, Sigma, cat. P4333), Glutamax (2 mM) (Gibco, cat. 35050038), and 5% fetal bovine serum (FBS) (Gibco, cat. 10270-106) at 36.5°C in 5% CO_2. Prior to ECM harvesting, fibroblasts were cultured for approximately five days until they reached confluency on culture plates. ECM was harvested as previously described (Chandrasekaran et al., 2021). Briefly, cells were washed with sterile nanopure water followed by 5 min incubation with 35 mM NH_4OH at room temperature (RT) at 750 rpm on a shaker for decellularization. Wells were then washed once with nanopure water, followed by 5 washes with DPBS. The plates were sealed with parafilm and stored in DPBS at 4°C until use for up to 4 weeks.

Differentiation of iPSCs into podocytes

iPSCs were differentiated into podocytes using an improved version of the protocol developed in our laboratory (Rauch et al., 2018; Murphy et al., 2019). The following changes were made: The final glucose concentration in the DMEM/F12 was reduced to 5 mM, which was achieved by combining DMEM (containing no glucose) and Ham's F-12 Nutrient Mix in a 1:1 ratio (Gibco, cat. 11966-025, Gibco, cat. 21765-029), and the seeding density of iPSCs for differentiation was adjusted to 22,000 cells/cm^2. In addition, FBS in the podocyte maintenance medium (to be used from day 11 onwards) was reduced from 2.5 to 1.25%.

In brief, iPSCs were detached with StemPro® Accutase® (Gibco, cat. A11105-01) and immediately plated out on the respective coatings in podocyte differentiation medium (DMEM, no glucose (Gibco, cat. 11966-025) with Ham's F-12 Nutrient Mix (Gibco, cat. 21765-029) (1:1) supplemented with 100 µM non-essential amino acids (NEAA) (Gibco, cat. 11140-050), penicillin-streptomycin (100 U/mL and 100 µg/mL, Sigma, cat. P4333), 2 mM Glutamax (Gibco, cat. 35050038), ITS (5 µg/mL insulin, 5 µg/mL transferrin and 5 ng/mL sodium selenite, Sigma, cat. I1884), 1.25% FBS (Gibco, cat. 10270-106), 15 ng/mL BMP7 (Gibco, cat. PHC9544), 10 ng/mL activin A (Stemcell Technologies, cat. 78001), and 100 nM retinoic acid (Merck, cat. R2625)). For seeding (day 0), Rho kinase inhibitor (Y-27632, ROCK inhibitor) was added at a concentration of 10 µM (Abcam, cat. 120129). Podocyte differentiation medium was renewed on day 1, day 3, day 6, day 9, and day 10 without ROCK inhibitor.

From day 11 onwards, podocytes were cultured in podocyte maintenance medium consisting of DMEM no glucose/HamF12 (1:1) containing 100 µM NEAA, penicillin-streptomycin (100 U/mL and 100 µg/mL), 2 mM Glutamax, ITS (5 µg/mL, 5 µg/mL and 5 ng/mL), and 1.25% FBS. To ensure a lower cell density for clear immunostaining, the cells were passaged at a ratio of 1:4 in a 24-well plate on day 12 with 10 µM ROCK inhibitor, then switched back to normal maintenance medium within 18-24 h and allowed to rest for 24 h before fixing with 4% paraformaldehyde (PFA).

Differentiation into iPSC-derived renal proximal tubular cells (PTL) and RPTEC/TERT1 culture

SFC086 or SBAD2 iPSCs were differentiated into PTL as previously described (Chandrasekaran et al., 2021) and fixed in 4% PFA on day 14.

RPTEC/TERT1 cells were obtained from Evercyte GmbH (Wieser et al., 2008) and cultured as previously described (Chandrasekaran et al., 2021). RPTEC/TERT1 were differentiated for 7 days prior to fixing in 4% PFA. Both cell types were used as negative controls for immunocytochemistry staining for podocytes and fibroblast markers, respectively.

Immunocytochemistry using high-content imaging (HCI) for pluripotency, fibroblast and podocyte markers

SFC086, SBAD3 and SBAD2 iPSCs were either grown in undifferentiated state or differentiated into podocytes on the commercial coatings (Geltrex, vitronectin, laminin-511, laminin-521) or on fibroblast-ECM. Undifferentiated cells were grown for at least 9 and 5 passages on commercial coatings and on fibroblast-ECM, respectively. Cells were fixed in 4% PFA in PBS, followed by 3 washes in PBS. Cells were blocked and permeabilized at RT for 30 min in PBS containing 5% bovine serum albumin (Sigma, cat. A9418-10G) and 1% Triton-X (Sigma, cat. T8787).

Undifferentiated cells were stained with the following primary antibodies: mouse monoclonal antibody POU5F1 (1:500) (Invitrogen, cat. MA1-104) and rabbit polyclonal antibody NANOG (1:200) (Invitrogen, cat. PA1-097x). fHDF/TERT166 and RPTEC/TERT1 were stained with rabbit monoclonal antibody Hsp47 (1:250) (abcam, cat. ab109117). Podocytes were fixed on day 14 of differentiation and stained with the following primary antibodies: rabbit monoclonal antibody synaptopodin (SYNPO) (1:75) (abcam, cat. ab224491) and goat antibody Wilms' tumor 1 (WT1) (1:100) (R&D Systems, cat. AF5729-SP568). For further characterization, SBAD2-derived podocytes differentiated on Geltrex were stained with the primary antibodies: rabbit polyclonal antibody nephrin (NPHS1) (1:100) (abcam, cat. ab183099) and rabbit polyclonal antibody Podocin (NPHS2) (1:100) (abcam, cat. ab50339). Primary antibody incubations were performed in 0.5% bovine serum albumin and 0.1% Triton-X for 1 h at RT or overnight at 4°C. Cells were then washed 3 times in PBS and incubated with corresponding secondary antibodies in 0.5% bovine serum albumin and 0.1% Triton-X for 35 min at RT: donkey anti-mouse Alexa 546 (1:500) (Invitrogen, cat. A10036), donkey anti-rabbit Alexa 488 (1:1000) (Invitrogen, cat. A21206) and Alexa Fluor 546 donkey anti-goat (1:250) (Invitrogen, cat. A1105). In addition, the nuclear stain Hoechst 33342 (1:10,000) (Invitrogen, Cat. H3570) was added to iPSCs, fHDF/TERT166, RPTEC/TERT1, and podocytes, and the F-actin stain phalloidin (ActinGreen™ 488 ReadyProbes reagent, Invitrogen, cat. R37110) was added to podocytes during incubation of secondary antibodies. Cells

were then washed 3 times in PBS, imaged on the Operetta CLS High Content Imager (PerkinElmer), and analyzed with Harmony 4.5 software version 3.10.6.

The total number of cells was determined by counting nuclei of Hoechst-stained cells. Ratio of NANOG-positive cells was calculated by dividing cells positive for NANOG staining by total cells counted. Two independent wells per iPSC line were analyzed, and a minimum of 5000 nuclei per condition were selected for the analysis.

Embryoid body differentiation from iPSCs and immunocytochemistry

SFC086, SBAD3 and SBAD2 iPSCs that had previously been cultured on the commercial coatings (Geltrex, vitronectin, laminin-511, laminin-521) or on fibroblast-ECM for a minimum of 10 and 5 passages, respectively, were differentiated into embryoid bodies (EBs) as previously reported (Wilmes et al., 2017). Briefly, cells were detached by incubation in 0.02% EDTA for 3 to 5 min at 36.5°C. Subsequently, iPSCs were resuspended in DMEM (Gibco, cat. 11966-025) and Ham's F12 Nutrient Mix Gibco (Gibco, cat. 21765-029) (1:1) medium containing 2 mM Glutamax (Gibco, cat. 35050038) and ITS (5 µg/mL insulin, 5 µg/mL transferrin and 5 ng/mL sodium selenite) and transferred (100 µL) to ultra-low attachment 96-well plates (without any additional coating) (CellCarrier Spheroid ULA 96 well Microplates, Perkin Elmar 6055330). Cells were fed carefully every two days by letting EBs sink to the bottom of the plate and replacing 70 µL of the medium with fresh medium. At day 7, the formed EB's of all conditions were transferred to CellCarrier-96 Ultra Microplates (Perkin Elmer 6055308) coated with Geltrex. EBs were fed every 2-3 days with 100 µL fresh medium until day 20 when they were fixed in 4% PFA in PBS.

Fixed EBs were stained with markers for the 3 germ layers using a 3-germ layer immunocytochemistry kit (Invitrogen, cat. A25538) according to the manufacturer's recommendations. The following primary antibodies were used: mouse IgG2a antibody smooth muscle actin (SMA) (A25531), rabbit antibody beta-III tubulin (TUJ1) (A25532), and mouse IgG1 antibody alpha-fetoprotein (AFP) (R&D systems, cat. RB01, which was not included in the 3-germ layer kit). The primary antibodies were incubated overnight at 4°C and washed 3 times followed by incubation with secondary antibodies Alexa fluor 488 goat anti-mouse IgG1, Alexa fluor 647 donkey anti-rabbit and Alexa Fluor 555 goat anti-mouse IgG2a (all included in the 3-germ layer kit) for 1 h at RT. EBs were washed 4 times with wash buffer, with the third wash containing the nuclear counterstaining NucBlue® Fixed cell stain/DAPI (1-2 drops/mL). EBs were imaged on Operetta CLS High Content Imager (PerkinElmer) and analyzed using the Harmony 4.5 software.

TempO-Seq sample preparation and analysis

SFC086, SBAD3 and SBAD2 undifferentiated iPSCs that had previously been cultured on the commercial coatings (Geltrex, vitronectin, laminin-511, laminin-521) or on fibroblast-ECM for a minimum of 15 and 5 passages, respectively, were cultured in 96-well plates until approximately 80% confluency. In addition, SBAD2 iPSCs were differentiated into podocytes in 24-well plates for 12 days. Cells were then washed once in PBS and incubated with 80 µL TempO-Seq lysis buffer (BioSpyder) in 96-well plates and 200 µL in 24-well plates for 15 min at RT. Plates were sealed and stored at -80°C until shipment to Bioclavis, Glasgow, United Kingdom for TempO-Seq analysis (Limonciel et al., 2018). Three replicates per undifferentiated iPSC line and 4 replicates for podocytes were analyzed. The quality of the resulting samples was checked for low read counts. All samples passed with a read count above 50,000 across all genes. The replicates were checked for outliers using Pearson's correlation coefficient. All passed the threshold of 0.80 under which they would have been removed. The raw data for all the samples was then analyzed using the R-based library DESeq2 (Love et al., 2014). Samples underwent an r-log transformation and posterior unsupervised clustering using standard DESeq2 suggested settings to visualize the variance within and among different coatings, cell lines, and differentiated cells. The raw data was then normalized using the standard mean-median ratio method in the DESeq2 library. These normalized rad counts were used to produce heatmaps of a selection of genes linked to pluripotent stem cells and podocytes based on the Scorecard gene panel and existing literature, respectively. The differential gene expression analysis among samples was performed using a DESeq2-based automatic script previously described in Singh et al. (2021) to generate fold changes (tested coating/Geltrex coating) with statistical values with thresholds that were set at a log-fold change of $> |0.56|$ and an adjusted $p > 0.05$.

Copy number variation via shallow DNA sequencing

SFC086, SBAD3 and SBAD2 undifferentiated iPSCs that had previously been cultured on the commercial coatings (Geltrex, vitronectin, laminin-511, laminin-521) or on fibroblast-ECM for a minimum of 12 and 5 passages, respectively, were washed once with DPBS followed by harvesting by 5 to 7 min incubation with 0.02% EDTA at 36.5°C. Cells were centrifuged for 5 min at 400 g at 4°C to collect cell pellets and washed once with DPBS before cell pellets were stored at -20°C. DNA isolation was performed using the QIAamp DNA mini kit (Qiagen, Cat. 51304) according to the manufacturer's instructions and including the optional step of incubation of samples with 40 µL RNase A (Sigma-Aldrich, cat. R6148) to achieve RNA-free DNA. Isolated DNA was sent to the Netherlands Cancer Institute (NKI, Amsterdam) for shallow sequencing of DNA. Low-coverage whole-genome samples, sequenced single-end 65 base pairs on the HiSeq 2500 were aligned to GRCh38 with bwa version 0.7.17, mem algorithm (Li, 2013). The mappability per 15 kilobases on the genome for a samples' reads, phred quality 37 and higher, was rated against a similarly obtained mappability for all known and tiled 65bp subsections of GRCh38, a reference genome-based mappability provided by QDNAseq (Scheinin et al., 2014), using a GRCh38 lifted version (Khan, 2020). QDNAseq segments data using an algorithm by DNA copy, and calls copy number aberrations using CGHcall (van de Wiel et al., 2007) and visualization was adapted from the QDNAseq code. These segments of potential copy number variations (CNV) were expanded from discrete genomic subsections, 15kb "bins", along the length of the

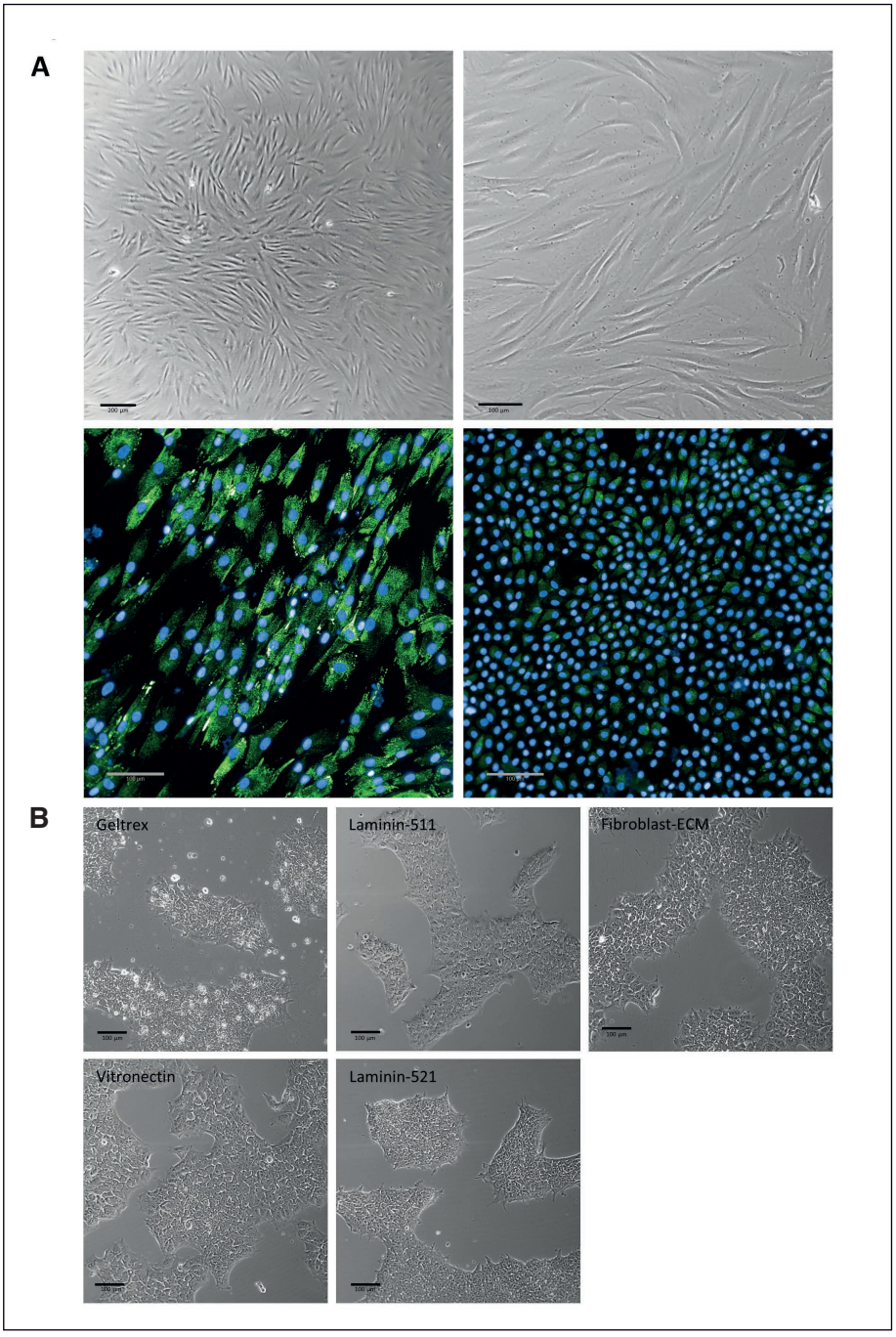

Fig. 1: Characterization of fibroblasts and colony formation of iPSC on different coatings
(A) Morphology and density of fibroblasts (fHDF/TERT166) for ECM harvesting are shown in the top panel at two magnifications. fHDF/TERT166 (bottom left) and RPTEC/TERT1 (bottom right) were stained for Hsp47 (green) and Hoechst 33342 (blue). (B) Morphology of iPSCs (donor: SFC086) on different coatings. Representative images based on three independent replicates are shown. Respective images for SBAD2 and SBAD3 are shown in Fig. S1[1].

chromosomes divided using BEDtools (Quinlan and Hall, 2010); CGHcall provided the segments. Segments that would indicate a copy number state change supported by less than 5% of the bins, and for a single sample, were excluded.

Statistical analysis

Statistical analysis for pluripotent staining of NANOG was carried out using one-way ANOVA with Dunnett's multiple comparison test (comparing all samples to Geltrex controls). For this, 6 replicates (two from each of the three different donors) were used. Statistical significance was considered for $p < 0.05$.

The normalized read counts for cells grown on all four alternative coatings were compared against those grown on Geltrex (using three replicates for each donor for each coating) for four important pluripotency related genes (*POU5F1*, *NANOG*, *Tra1-60* and *KLF4*) using one-way ANOVA with Dunnett's multiple comparison test (comparing all samples to Geltrex controls). Statistical significance was considered for $p < 0.05$..

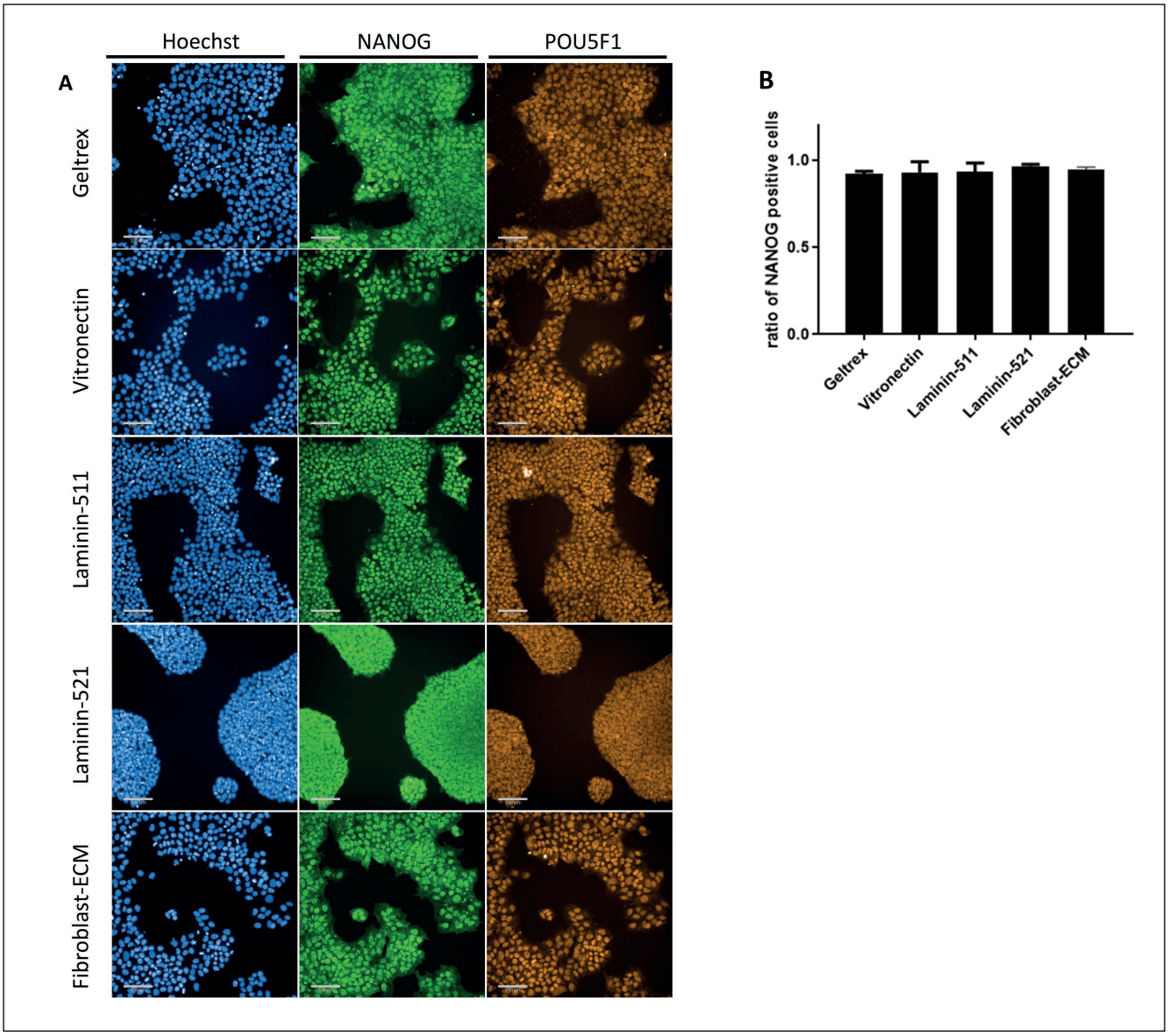

Fig. 2: Pluripotent marker staining of SBAD2 iPSC

(A) Representative images of iPSC stained with Hoechst 33342 (blue) and antibody staining with NANOG (green) and POU5F1 (orange) based on two independent replicates per donor are shown. Scale bar represents 100 μm. (B) Percentage of cells stained with the pluripotent marker NANOG. SBAD2 were cultured on respective coatings and stained with Hoechst 33342 and NANOG. Ratio of cells expressing NANOG compared to total cells (Hoechst 33342) is shown for 6 replicates (2 replicates of each iPSC donor) with at least 5000 nuclei analyzed. Statistical analysis was performed using a one-way ANOVA, comparing all coatings to Geltrex (control). No significant difference ($p < 0.05$) was observed. Respective images for SBAD3 and SFC086 are shown in Fig. S2[1].

3 Results

3.1 Comparison of cell growth and pluripotent markers on different coatings

Human foreskin fibroblasts (fHDF/TERT166) showed a typical fibroblast morphology and high expression levels of the dermal fibroblast marker HSP47. Renal proximal tubular cells (RPTEC/TERT1) were used as a negative control and showed only minor HSP47 expression levels (Fig. 1A). Prior to ECM harvesting, fibroblasts were cultured to confluency as seen in Figure 1A.

Here, we cultured three different hiPSC lines for at least 9 and 5 passages for commercial and fibroblast-ECM, respectively. Cell attachment of all three hiPSC lines on fibroblast-ECM and all commercial coatings worked equally well, and no apparent difference in growth rates was observed (data not shown). The expression of pluripotent markers is an important hallmark of

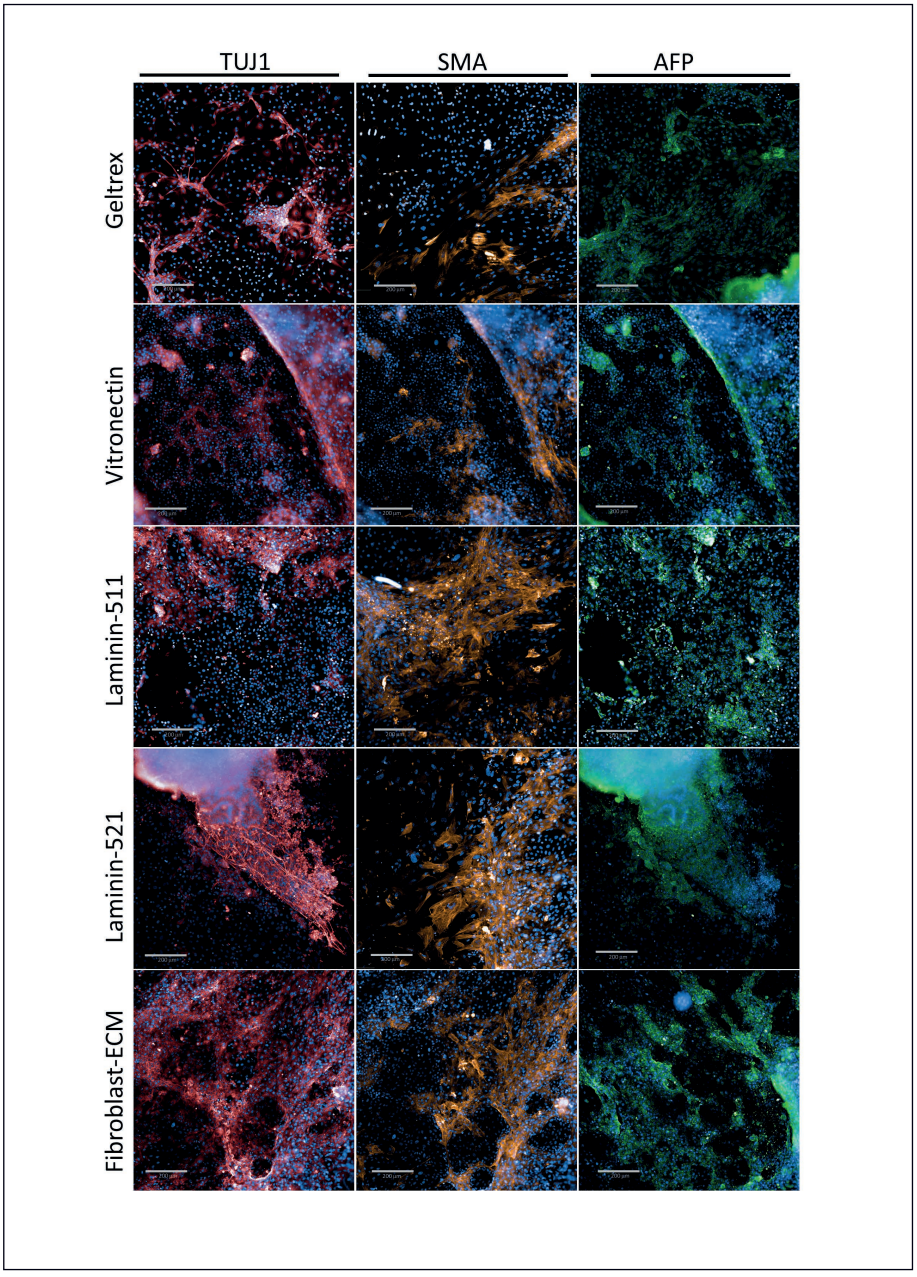

Fig. 3: Embryoid bodies (EBs) derived from SBAD2 iPSC
EBs were fixed and imaged after 3 weeks. Antibody staining for the ectoderm marker TUJ1 (red), the mesoderm marker SMA (orange), and the endoderm marker AFP (green) are shown. Nuclear staining was performed with DAPI (blue). Scale bar represents 200 μm. EB were obtained from at least 3 replicates per coating. Results show representative images based on three independent replicates. Respective images for SBAD3 and SFC086 are shown in Fig. S3[1].

iPSCs and should be carefully monitored as a quality control for each generated iPSC line. The pluripotent markers POU5F1 and NANOG were analyzed via HCI and showed typical nuclear staining patterns (Fig. 2A; Fig. S2[1]). To quantify the number of cells that stained positive with NANOG, positively stained cells and total cells (stained with Hoechst 33342) were counted with the Harmony software of the HCI and expressed as ratio of NANOG/Hoechst (Fig. 2B). All three alternative commercial coatings as well as the in-house produced ECM-coating showed a similar staining pattern compared to animal-derived Geltrex™ in the three different iPSC lines. The number of NANOG positive cells was high in cell lines cultured on all coatings, with values ranging from 85-99%, and no significant differences compared to Geltrex were observed.

3.2 Differentiation into embryoid bodies (EBs)

Another important key characteristic of iPSCs is their ability to differentiate into all three germ layers, namely ectoderm, mesoderm, and endoderm. This quality control also should be carefully monitored after the generation of new iPSC lines. We examined the differentiation of three hiPSC lines into EBs after prolonged culture time on alternative coatings. For this, iPSCs were cultured for a minimum of 10 and 5 passages for commercial and fibroblast-ECM, respectively, and differentiated into EBs as previously

described (Wilmes et al., 2017). After 3 weeks, EBs were fixed and stained with antibodies representing the three germ layers, including TUJ1 (ectoderm), SMA (mesoderm), and AFP (endoderm), and imaged on the HCI (Fig. 3; Fig. S3[1]). We observed that hiPSCs grown on all alternative coatings were able to differentiate into EBs equally well compared to hiPSCs grown on Geltrex. EBs showed a typical morphology of neuronal-like structures with TUJ1 staining, muscle fiber-like structures with SMA staining, and small cytoplasmic staining patterns with AFP staining.

3.3 Genome-wide transcriptomics analysis of hiPSCs on different coatings

Genome-wide transcriptomics was carried out with TempO-Seq[2]. Read counts of all gene probes were normalized with DESeq2 and underwent clustering analysis with principal component analysis (PCA). Undifferentiated iPSCs clustered closely together and well apart from iPSC-derived podocytes (Fig. 4A). Most variability was observed across donors, with two donors (SBAD3 and SFC086) clustering together and one donor (SBAD2) clustering separately; however, separation between them was relatively small (below 5% difference). It was noted that the cell lines clustering closer together were from female donors, whereas the other line was from a male donor; however, no further characterization of sex-related differences was carried out as this was beyond the scope of this study.

In terms of clustering among different coatings, relatively low separation of samples was retrieved, indicating relatively high overall similarity for all coatings. To look more into cell type-specific gene expression, we used the pluripotent genes that are present in the Scorecard assay (Fergus et al., 2016) for undifferentiated iPSCs. These pluripotent genes were presented in form of a heat map, where red and blue colors represent the highest and lowest mRNA expression per row, respectively, and the values represent the average read counts of three biological replicates (Fig. 4B). iPSCs expressed high levels of pluripotent genes for all coatings. At the single gene level some differences were observed, with sometimes alternative coatings showing slightly higher and sometimes slightly lower expression levels compared to Geltrex, e.g., cells cultured on vitronectin or ECM coatings had the highest expression levels across coatings for *CXADR* and *LIN28A* or for *KLF4* and *SALL4*, respectively, whereas cells grown on laminin-511 and laminin-521 showed the highest expression levels across coatings for *LIN28B* and *ZIC5* or *ZFP42*, respectively. On the other hand, cells grown on Geltrex coatings showed highest expression levels of *PODXL* and *POU5F1*. However, no clear trend was observed that indicated that one coating was always lower for all pluripotent genes.

In addition to the heat map, selected pluripotent markers that are most frequently reported for pluripotent genes (*NANOG*, *POU5F1*, *PODXL* and *KLF4*) were graphed in bar charts in Figure 4C. No significant difference was observed for *NANOG* mRNA expression in iPSCs cultured on vitronectin, laminin-521 or fibroblast-ECM compared to Geltrex, and levels were slightly lower in iPSCs cultured on lamin-511 for two of the three tested iPSC-lines. Read counts for *POU5F1* were slightly lower for iPSCs cultured on vitronectin (for 2 out of 3 tested cell lines), laminin-511 (all three cell lines tested), laminin-521 (for 2 out of 3 tested cell lines), and for fibroblast-ECM (for 1 out of 3 tested cell lines). It should be noted though that overall expression levels of both *NANOG* and *POU5F1* were high for all conditions compared to non-pluripotent cells such as the podocyte-like cells (Fig. 4B). *PODXL* expression levels were slightly lower in all three cell lines when cultured on laminin-511 and laminin-521, and for one of the three tested cell lines cultured on vitronectin or fibroblast-ECM. *PODXL* is also highly expressed in iPSC-derived podocytes, which is in line with expression levels of renal podocytes *in vivo*. *KLF4* expression levels were not significantly reduced in any conditions; in fact, they were increased in iPSCs cultured on fibroblast-ECM in all three cell lines.

3.4 Genomic stability of hiPSCs on different coatings

Shallow DNA sequencing was performed to monitor long-term effects on karyotype after culturing of hiPSCs on alternative coatings and Geltrex for a number of passages. For this, three different iPSC lines were cultured for a minimum of 12 and 5 passages on commercial and fibroblast-ECM, respectively. We did not observe any large chromosomal aberrations for any of the tested coatings. Minor copy number variations (CNVs) were observed, with aberrations above 2 megabase pairs (Mbp) seen on chromosomes 1, 3 and 20 (Fig. 5A-C). It was interesting that the main effects seemed to be cell line-specific rather than an effect of the prolonged culture on the coatings, with SFC086 showing the fewest events of CNVs, ranging from 1 to 4 events, compared with 3 to 5 and 3 to 6 events for SBAD3 and SBAD2, respectively (Fig. 5E). It should be noted though that total passage numbers before switching to alternative coatings were lower for SFC086 than for SBAD2 and SBAD3 (DNA sequencing was carried out at passage 32 compared to passage numbers 49, respectively, on all commercial coatings). Nevertheless, the total length of deletions was slightly higher for SFC086 (maximum of 2.18 Mbp) compared to SBAD2 (maximum of 1.16 Mbp) and SBAD3 (maximum of 0.48 Mbp). The total lengths of duplications were highest in SBAD3 (maximum of 6.96 Mbp) followed by SFC086 (maximum of 3.26 Mbp) and SBAD2 (maximum of 1.52 Mbp) (Fig. 5D). A summary of CNVs per coating is given in Figure 5D. CNVs of hiPSC grown on vitronectin, laminin-511, and fibroblast-ECM were similar or slightly lower than CNVs of respective cell lines grown on Geltrex. hiPSCs grown on laminin-521 showed slightly higher CNVs compared to respective cell lines grown on Geltrex; however, overall CNVs were still relatively low.

3.5 Differentiation of iPSCs into podocyte-like cells

The three hiPSC lines were differentiated into podocyte-like cells on the commercial coatings and fibroblast-derived ECM and compared to podocyte differentiation on Geltrex. Podocyte-like

2 doi:10.14573/altex.2112204s2

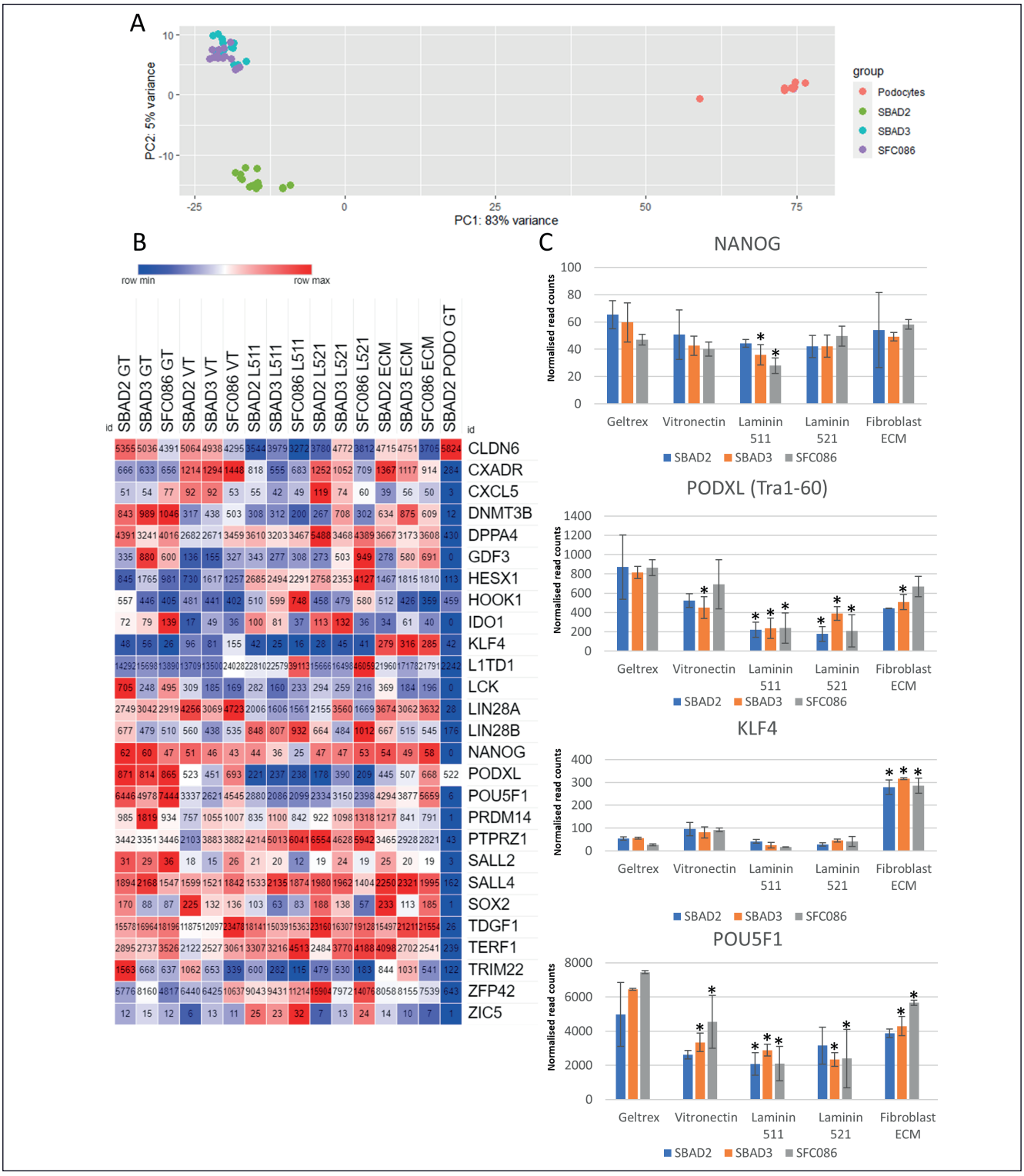

Fig. 4: TempO-Seq analysis of pluripotent genes from 3 iPSC cell lines cultured on different coatings

(A) Principal component analysis (PCA) clustering plot of three undifferentiated iPSC lines (SBAD2, SBAD3 and SFC086) and iPSC-derived podocyte-like cells (negative control) on different coatings. (B) Heatmap of selected pluripotent stem cell-related genes for the average (from three replicates per cell line) normalized read counts for each iPSC cell line on different coatings. Podocyte-like cells grown on Geltrex served as a negative control. Dark red and blue colors represent the highest and lowest gene expression levels per row, respectively. (C) Four important pluripotent markers are presented as bar graphs. Statistical analysis was performed with one-way ANOVA with Dunnett's multiple comparisons test compared to Geltrex (control). *, $p < 0.05$, $n = 3$.

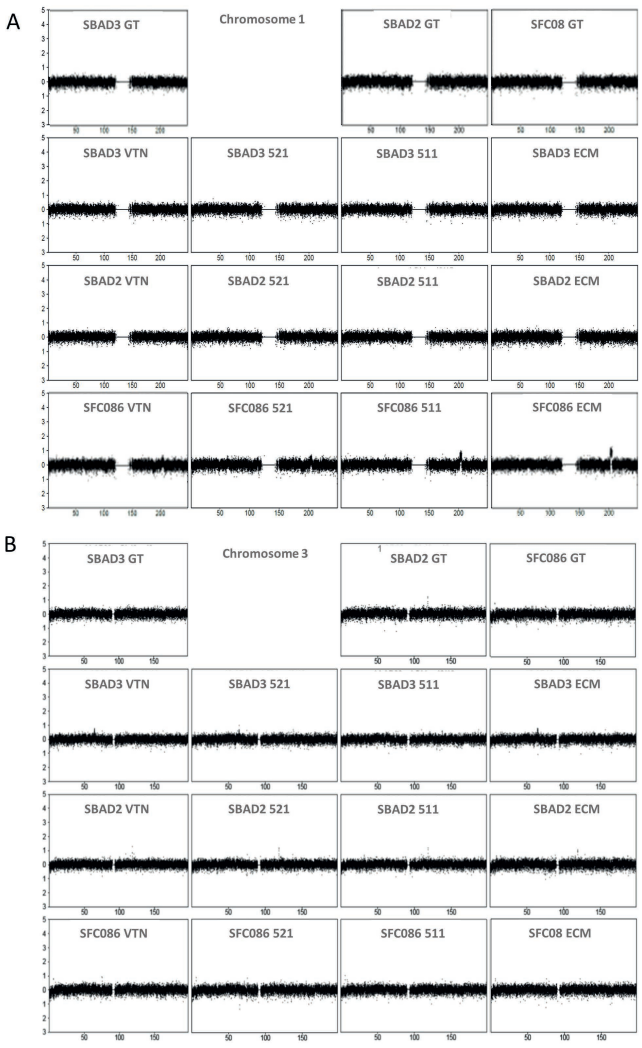

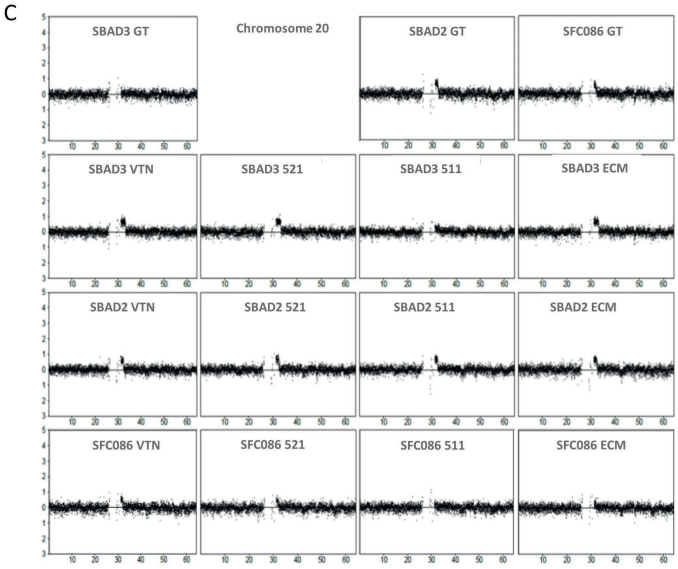

D

Total length of deletions (in Mbp)			
	SBAD2	SBAD3	SFC086
Geltrex	1.10	0.42	0.08
Vitronectin	0.29	0.42	0.05
Laminin-511	1.16	0.45	2.19
Laminin-521	0.83	0.48	0.17
Fibroblast-ECM	0.08	0.42	0.18

Total length of duplications (in Mbp)			
	SBAD2	SBAD3	SFC086
Geltrex	1.23	0.00	0.00
Vitronectin	1.29	0.38	3.26
Laminin-511	1.22	6.96	3.23
Laminin-521	1.34	0.00	3.18
Fibroblast-ECM	1.52	2.45	3.18

Number of copy number variations (homozygous)			
	SBAD2	SBAD3	SFC086
Geltrex	6(2)	3(2)	1(0)
Vitronectin	5(2)	3(1)	2(0)
Laminin-521	6(3)	5(1)	3(1)
Laminin-511	6(1)	3(2)	4(1)
Fibroblast-ECM	3(0)	4(1)	4(0)

cells were either fixed and stained with podocyte-specific markers or lysed for TempO-Seq for one of the cell lines (SBAD2).

All alternative coatings produced podocyte-like cells that stained positive with synaptopodin and WT1 (Fig. 6A; Fig. S4A, B[1]) and were comparable to podocyte-like cells cultured on the animal-derived Geltrex coating. No adaptations, e.g., changes in seeding densities or adjustment of concentrations of growth factors, were required compared to the differentiation protocol on Geltrex.

iPSC-derived podocytes from one donor (SBAD2) were used for comparison of two of the alternative coatings, laminin-521 and fibroblast-ECM, to Geltrex via genome-wide transcriptomics analysis using TempO-Seq. PCA plot showed that all podocyte-like cells from all conditions clustered together and well apart from undifferentiated iPSCs (Fig. 4A).

For analysis of podocyte-specific markers, we selected genes from previously published single-cell RNASeq experiments, including data of primary mouse podocytes (Lu et al., 2017) and human tissue (Lake et al., 2019). We observed a remarkably high similarity of mRNA expression of podocyte-related genes among all three coatings (Fig. 6B). In addition to heat maps, selected podocyte-specific markers were displayed as bar charts (Fig. 6C). High levels of most podocyte-related markers were observed across all coatings, including *CLIC5 PLA2R1*, and *PODXL*. Slightly lower expression levels of *PALLD* and *COL4A3* were observed for podocyte-like cells differentiated on laminin 521 and for *VEGFA* for podocyte-like cells differentiated on fibroblast-ECM.

Surprising low or no mRNA expression was detected for probes for *SYNPO*, *NPH1*, *NPH2* and *WT1* for all coatings, including Geltrex, despite all of them being expressed at the protein levels as seen in Figure 7 and Figure S5[1]. Protein expression of all four markers, as well as mRNA expression of *SYNPO*, had also been reported in our previous study in podocyte-like cells differentiated on Geltrex (Rauch et al., 2018).

E

			SBAD2					SBAD3					SFC086				
Chromsome	Start	End	GT	VTN	L-521	L-511	ECM	GT	VTN	L-521	L-511	ECM	GT	VTN	L-521	L-511	ECM
1	2.02E+08	2.05E+08	.	.	.	.	.	.	.	.	.	.	.	DUP (CN3)	DUP (CN3)	DUP (CN3)	DUP (CN3
10	52065000	52230000	DEL (CN1)	DEL (CN0)	DEL (CN1)	DEL (CN1)	.	.	.	.	.	.	.	.	.	.	.
12	11355000	11400000	.	.	.	.	.	.	.	DEL (CN1)	.	.	.	DEL (CN1)	.	DEL (CN1)	DEL (CN1
14	41145000	41190000	.	.	.	.	.	.	.	.	.	.	.	.	.	DEL (CN1)	.
19	53835000	53895000	.	DUP (CN3)	.	.	DUP (CN3)	.	.	.	.	.	.	.	.	.	.
2	1.65E+08	1.65E+08	.	.	.	DUP	.	.	.	.	.	.	.	.	.	.	.
2	1.84E+08	1.84E+08	.	DEL (CN0)	DEL (CN1)	DEL (CN1)	.	.	.	.	.	.	.	.	.	.	.
20	32280000	32445000	DUP (CN3)	DUP (CN3)	DUP (CN3)	DUP (CN3)	DUP (CN3)	.	.	DUP (CN3)	.	DUP (CN3)	.	.	.	.	.
22	33540000	33900000	.	.	.	.	.	DEL (CN0)	DEL (CN0)	DEL (CN0)	DEL (CN0)	DEL (CN1)	.	.	.	.	.
3	64755000	65130000	.	.	.	.	.	.	DUP (CN3)	DUP (CN3)	.	DUP (CN3)	.	.	.	.	.
4	34785000	34830000	DEL (CN1)	.	DEL (CN1)	.	.	.	DEL (CN1)	DEL (CN1)	DEL (CN1)	DEL (CN1)	.	.	.	.	DEL (CN1
6	78270000	78330000	DEL (CN1)	DEL (CN1)	DEL (CN0)	DEL (CN1)	DEL (CN1)	.	.	.	.	.	DEL (CN1)	.	DEL (CN0)	DEL (CN0)	DEL (CN1
7	9030000	9090000	.	.	.	.	.	DEL (CN0)	.	.	DEL (CN0)	.	.	.	.	.	.
7	74205000	74220000	DEL (CN0)	.	DEL (CN0)	DEL (CN0)	.	.	.	.	.	.	.	.	.	.	.
7	1.33E+08	1.33E+08	.	.	.	.	.	DEL (CN1)	.	.	.	.	.	.	.	.	.
9	1.04E+08	1.04E+08	DEL (CN0)	.	DEL (CN0)	.	.	.	.	.	.	.	.	.	DEL (CN1)	.	.

Fig. 5: Karyotyping of iPSC cultured on different coatings

SBAD2, SBAD3 and SFC086 were cultured on commercial coatings (GT: Geltrex, VTN: vitronectin, 511: laminin-511 and 521: laminin-521) for 15, 13 and 12 passages respectively and on fibroblast-ECM for 5, 6 and 6 passages respectively. Shallow DNA sequencing was performed to identify copy number variations (CNV). The three chromosomes with the most abundant CNV are shown in (A) (Chromosome 1, 3.18 Mbp), (B) (Chromosome 3; 4.89 Mbp) and (C) (Chromosome 20; 2.07 Mbp). Total CNVs across all chromosomes are summarized in (D). Table of locations of deletions (CN1:heterozygous and CN0:homozygous) and duplications (CN3) is shown in (E). Samples were from one replicate per condition (i.e., 5 replicates per cell line).

We compared podocyte-specific gene expression between our original protocol as described in Rauch et al. (2018) with the modified protocol described here. In the adjusted, current protocol the amount of glucose present in the medium was lowered from 17.5 mM to 5 mM to represent more physiological conditions. The gene expression profile was comparable between both protocols (Fig. S5[1]), with only very few podocyte-specific genes being mildly increased (including *VEGFA*, *PALLD*, *PLA2R1*, *COL4A3*, *LAMB2*, *CD59* and *ROBO2*) or mildly decreased (including *CDK1C*, *CLIC5* and *ENPEP*) in the new low-glucose protocol.

3.6 Differentiation of iPSCs into renal proximal tubular cells (PTL)

To evaluate how these different coatings perform for differentiation into another cell type, we differentiated SBAD2 iPSCs into PTL. In addition to the coatings mentioned above, we also tested ECM generated by the proximal tubular cell RPTEC/TERT1, as previously described (Chandrasekaran et al., 2021). We observed no apparent difference in morphology or staining patterns with the proximal tubular marker megalin and the tight junction marker ZO3 when cells were differentiated on either of the decellularized ECM-coatings compared to Geltrex (Fig. S6[1]). Nevertheless, not all single protein coatings worked equally well for PTL differentiation. Vitronectin coating performed the worst, with differentiating PTL cells not forming a confluent monolayer and exhibiting holes (data not shown). Furthermore, the areas where cells attached showed less consistency with cell morphology, indicating presence of other cell types, as well as less polarization of the cells as observed by largely cytoplasmic rather than tight junction expression patterns of ZO3 (Fig. S6[1]). Both laminin coatings produced confluent monolayers of PTL cells, but also showed slightly less polarization observed by ZO3 staining, with laminin 521 looking better than laminin 511 (Fig. S6[1]).

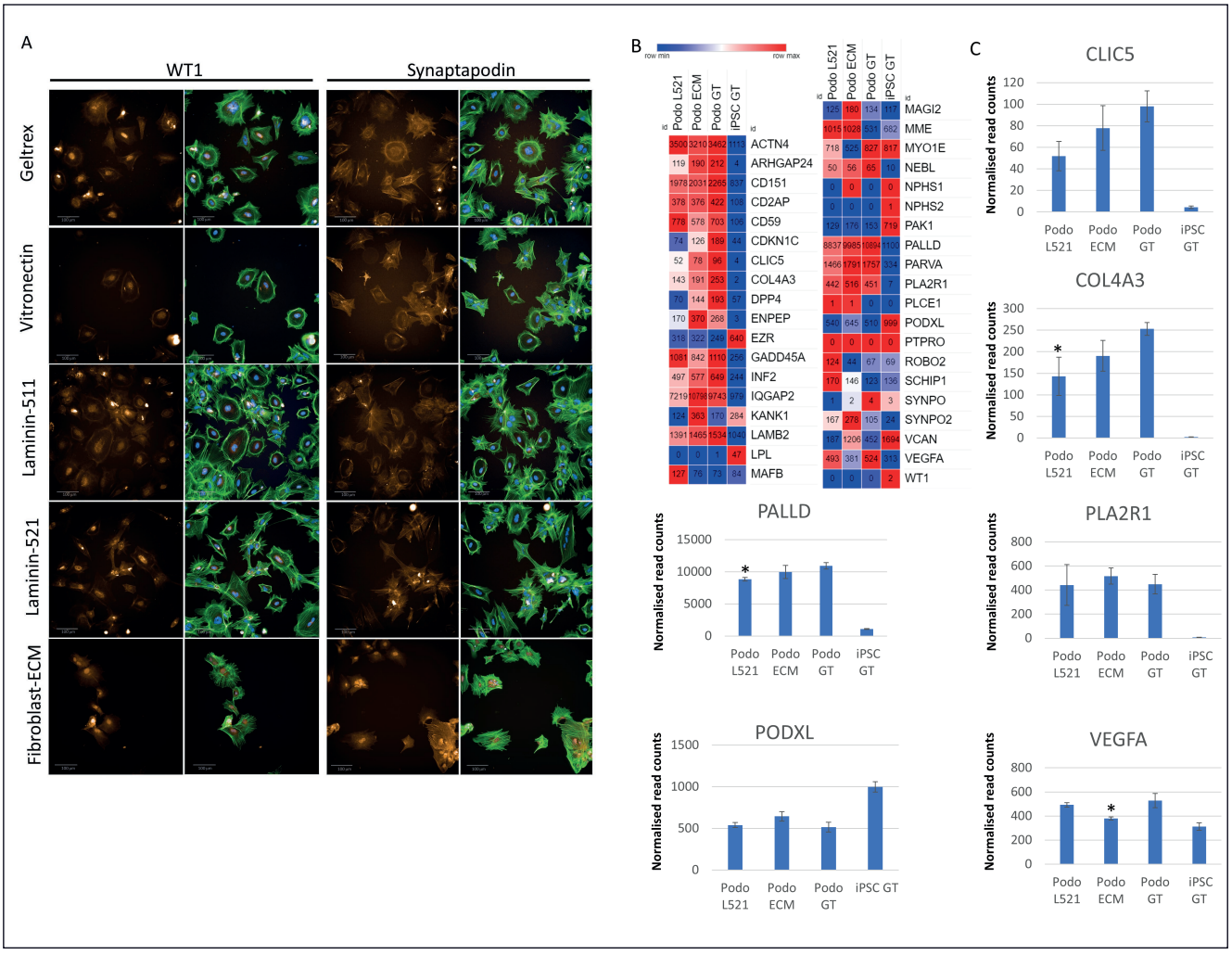

Fig. 6: Podocyte-specific markers upon iPSC differentiation into podocyte-like cells on different coatings
(A) SBAD2 were differentiated into podocyte-like cells on different coatings and stained on day 14 with the podocyte markers WT1 and synaptopodin (orange), and with phalloidin (staining f-actin, green). Nuclear staining was performed with Hoechst 33342 (blue). Left panel shows antibody staining alone and right panel shows antibody staining overlay with phalloidin and Hoechst 33342. Images shown are representative images based on three independent replicates. (B) TempO-Seq analysis of podocyte-related genes for podocyte-like cells grown on different coatings. Heatmap of a range of podocyte-related genes for the average normalized read count for iPSC derived podocyte-like cells, generated from the SBAD2 iPSC cell line differentiated on Geltrex (GT), laminin-521 (L521) and fibroblast-ECM (ECM) with undifferentiated SBAD2 iPSCs grown on Geltrex for comparison. Values resemble average of four replicates. Dark red and blue colors represent the highest and lowest gene expression levels per row, respectively. (C) Selected podocyte markers are presented as bar graphs. Statistical analysis was performed with one-way ANOVA with Dunnett's multiple comparisons test comparing podocyte-like cells on alternative coatings to Geltrex (control). *, $p < 0.05$, $n = 4$. Respective images for SBAD3 and SFC086 are shown in Fig. S4[1].

4 Discussion

There are many reasons for replacing the use of animal-derived Matrigel® for hiPSC maintenance or iPSC differentiation, including batch-to-batch variations, using non-human material, and ethical concerns about its production. In a proteomic study by Hughes et al. (2010), 1851 proteins were identified in several batches of Matrigel, with a batch-to-batch similarity as low as 53%. While there are some commercially available alternatives, these are often only tested or recommended for use with very specific culture media (e.g., Vitronectin in combination with E8 medium). Furthermore, different morphological appearance of hiPSCs on some of these alternative coatings and limited comparison studies may cause concerns and hinder a broader uptake of these alternative coatings. Lastly, the often higher price of recombinant proteins may influence the choice of coating used in hiPSC culture. In this study we performed an extensive and deep characterization, including whole genome TempO-Seq transcrip-

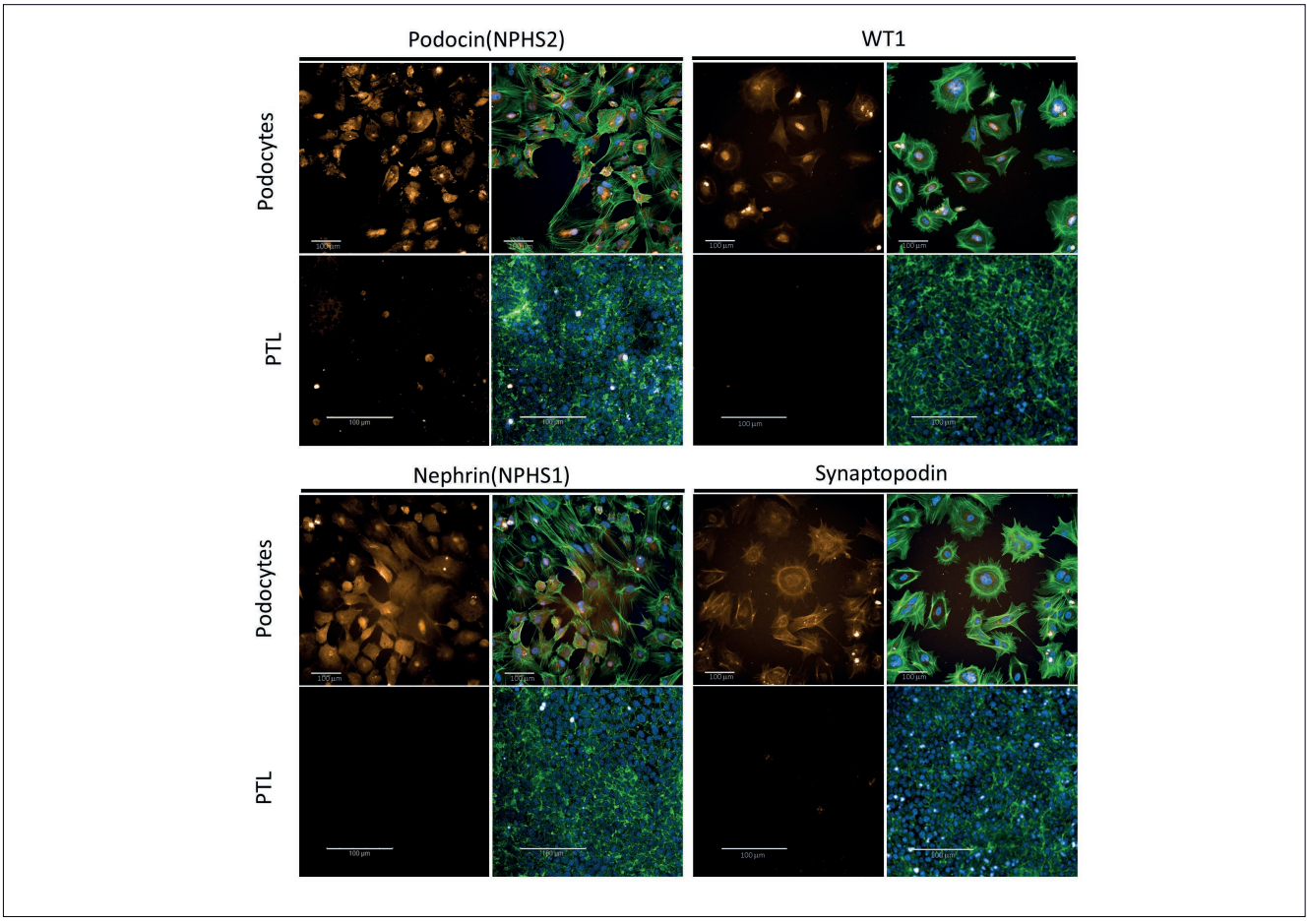

Fig. 7: Podocyte-specific markers with negative controls

iPSC-derived podocyte-like cells (donor SBAD2) and iPSC-derived renal proximal tubule-like cells (PTL, negative control, donor SFC086) were stained with the podocyte markers podocin (NPHS2), nephrin (NPHS1), WT1, and synaptopodin (orange), and with phalloidin (staining f-actin, green). Nuclear staining was performed with Hoechst 33342 (blue). Left panel shows antibody staining alone and right panel shows antibody staining overlay with phalloidin and Hoechst 33342. Representative images are shown that are based on three independent replicates.

tomics and karyotype analysis (CNVs) using shallow DNA sequencing, to compare different commercial coatings for three iPSC lines cultured for a minimum of nine passages under identical cell culture medium conditions. In addition, we produced a low-cost human fibroblast-ECM coating in-house that was tested with three hiPSC lines cultured for a minimum of 5 passages on this new coating.

4.1 iPSC characterization

Following their switch to the respective alternative coatings, hiPSCs from all three lines grew well and showed a consistent iPSC-characteristic morphology (Fig. 1B; Fig. S1[1]), growing in colonies with distinct edges (Nagasaka et al., 2017). Pluripotent markers were analyzed in a genome-wide screen at the mRNA level and with antibody staining for two markers, POU5F1 and NANOG, sometimes referred to as the "master genes" of pluripotency (Pan and Thomson, 2007), at the protein level. Looking at mRNA levels from the panel used in the Scorecard assay for functional pluripotency (Tsankov et al., 2015), we saw generally high and similar expression of these genes across all coatings (Fig. 4B). While there seemed to be a minor but significant difference in *NANOG* and *POU5F1* at mRNA expression levels for some of the alternative coatings, this could not be observed at the protein level as immunofluorescence staining for POU5F1 and NANOG showed no apparent differences in staining intensity or percentage of positively stained cells throughout the colonies on all the coatings (Fig. 2). A typical nuclear staining was observed for NANOG (Hyslop et al., 2005) (Fig. 2B), while POU5F1 is primarily localized in the nucleus, but also shuttled back and forth into the cytoplasm (Young et al., 2011), which was also observed in the current study. This suggests that the TempO-Seq transcriptomics study showed a much higher sensitivity to pick up more subtle differences. Nevertheless, whether these subtle differences

at mRNA level are of importance in terms of protein function is questionable, in particular as all observed read counts for *POU5F1* and *NANOG* across all coatings were in general quite high compared to read counts in differentiated podocyte-like cells that served as a negative control. The majority of pluripotent markers in iPSC-derived podocytes showed low to no mRNA expression. Two exceptions were *PODXL* and *KLF4*, which both showed clear expression that remained consistent across all coating in the podocyte-like cells. This is expected as both genes play important roles in the formation and function of podocytes (Refaeli et al., 2020; Pace et al., 2021). Interestingly, *KLF4*, one of the Yamanaka factors used for the reprogramming of iPSCs (Takahashi and Yamanaka, 2006), showed a much higher difference in mRNA expression levels in undifferentiated iPSCs, with a significantly greater expression for all three cell lines when cultured on fibroblast-ECM compared to any of the other coatings, including Geltrex™ (Fig. 4). The implications of such increased expression levels remain unclear but given the number of important functions KLF4 has been found to play in the upkeep of stem cell pluripotency, including the regulation of *NANOG* (Zhang et al., 2010), it is more likely to have a positive rather than negative impact on the pluripotency of these cells.

Moreover, we noticed a donor-specific expression profile that was independent of the different coating used. The cell line SFC086 showed overall higher levels of mRNA for several pluripotent markers compared to the other two lines. This may be related to the lower passage of this cell line number prior to the transfer to alternative coatings. Nevertheless, this is speculative and not consistent across all markers (Fig. 4B), as there were also key pluripotent genes, including *NANOG* and *KLF4*, that showed higher levels in the other cell lines.

In addition to the comparison to the well-established pluripotent panel within the Scorecard assay, we were also interested in analyzing our samples in an unbiased approach to potentially identify any gene changes that were induced after prolonged culturing on the respective coatings. For this, DESeq2 analysis was used to compare differentially expressed genes between the Geltrex coating control and respective alternative coatings. The top 50 most up- or down-regulated genes in comparison to Geltrex are shown in Table S2[1], most of which were not related to cell pluripotency, cell growth or attachment. Several differentially expressed genes appeared to be impacted by the different coatings across cell lines, including, as mentioned above, a significant up-regulation of *KLF4* in all cell lines grown on fibroblast-ECM. Additionally, hiPSCs grown on vitronectin and fibroblast-ECM shared a number of upregulated genes, including several MT1 and MT2 isotypes, *Dap3*, *CD24* and *SPP1*. Of these, the most interesting seemed the MT1 and MT2 isotypes that belong to the groups of metallothioneins, important metalloregulators that have been previously reported to have the potential to impact the stability and maintenance of iPSCs (Lu et al., 2018). In one study, metallothioneins have been reported to play a role in the transport of zinc into the nucleus, which has been suggested to negatively impact pluripotency (Wolford et al., 2010). However, metallothioneins, particularly MT1 isotypes, have been reported to be enhanced in protein-protein networks important in pluripotent cells (Slamecka et al., 2018).

Lastly, the capacity of hiPSCs to be differentiated into EBs was tested to demonstrate their pluripotent nature upon prolonged culturing on alternative coatings. Spontaneous differentiation into EBs, followed by analysis of markers for meso-, endo-, and ectoderm, could be clearly observed in all the samples (Fig. 3; Fig. S3[1]). The physicochemical properties of ECM may have a large impact in directing the differentiation of stem cells *in vivo*, by directing them towards certain lineages while closing off others (Padhi and Nain, 2020). Therefore, this retention of their pluripotent capabilities over repeated passages on these alternative coatings supports the view that they can be used for the longer-term culture of iPSCs that maintain their stability and utility as a potential source of cells from all three germ-layers.

4.2 iPSC genetic stability

Genomic stability and a normal karyotype are desired for any iPSC line and considered as one of the many advantages of iPSCs over cancer cell lines that often show an abnormal karyotype. Ideally, only iPSC clones with a normal karyotype in terms of chromosomal numbers are selected after reprogramming; however, more subtle genomic alterations that are not detected by Giemsa staining karyotyping often exist in iPSC. Within the Human Induced Pluripotent Stem Cells Initiative (HipSci), 711 iPSCs were analyzed for genomic stability and 41% of iPSC lines contained at least one or several copy number variations (CNVs) with an average of 7.15 Mb in length (Kilpinen et al., 2017). While duplications or deletions of entire chromosomes should be avoided at all costs, more subtle changes at CNVs of genes may be unavoidable. Other researchers have reported increased levels of CNVs in iPSCs in response to different types of cell culture conditions or different passaging methods, including increased CNVs after acidification of cell culture medium due to high density cultures (Jacobs et al., 2016) or increased CNVs due to enzymatic passaging with Accutase (Garitaonandia et al., 2015). Moreover, differences in CNVs have been observed in response to culturing iPSCs on feeder cells compared to Matrigel (Garitaonandia et al., 2015).

Therefore, we investigated whether prolonged culturing of iPSCs on the new alternative coatings had any impact on CNVs or even entire chromosomes. In this study, overall, no major chromosomal aberrations were observed for any conditions and all hiPSCs showed a normal number of chromosomes. Furthermore, the total number of CNVs in all the samples was either comparable to, or far below, the averages seen in the Kilpinen study for all tested coatings (Fig. 5A-C,E). When looking at the specific CNVs occurring in each sample (Fig. 5B), no clear trend linking any increased instability to one of the tested coatings could be seen. More frequently CNVs were shared among most or all of the samples from one of the donors regardless of sample, suggesting this alteration is more a pre-existing feature of the cells than an impact of a new coating. Of the CNVs observed, most impacted

relatively few genes or non-coding areas. These were generally seen only within the same cell line (Fig. 5E), indicating that they are unlikely the result of culture on any of the tested coatings.

4.3 Podocyte differentiation

Consistent and reliable differentiation into a desired cell type is essential for hiPSC work. To further assess the performance of these alternative coatings compared to Geltrex for directed hiPSC differentiation, an established protocol based on the on-step differentiation into renal podocyte-like cells (Rauch et al., 2018) was performed using hiPSCs from all three lines. This protocol was chosen based on its relatively short differentiation time, clear morphological change, and experimenter familiarity. hiPSCs were cultured on Geltrex prior to differentiation on each of the five tested coatings. Coating of the plates was essential for the initial days of differentiation into podocyte-like cells, in contrast to seeding out fully differentiated podocyte-like cells after subculture, which did not require coated wells, presumably as the fully differentiated podocytes were able to produce their own ECM. In addition to initial attachment, the composition of the coating may influence the differentiation procedure, as the ECM is also involved in signaling interactions with the cells (Padhi and Nain, 2020).

Differentiation of hiPSCs into renal podocyte-like cells appeared very consistent across all four alternative coatings for all three cell lines, with the post-differentiation podocytes displaying their characteristic large size and foot process-like appendages, as seen in the podocyte actin staining (Fig. 6A,7; Fig. S4[1]). All conditions showed clear antibody staining against commonly used podocyte-specific proteins, including synaptopodin and WT1, which were particularly localized to the cytoskeleton and nucleus, respectively (Fig. 6A; Fig. S4A-B[1]). Surprisingly, this contrasted with mRNA levels for synaptopodin (*SYNPO*) and *WT1*, as well as two other characteristic podocyte markers, nephrin (*NPH1*) and podocin (*NPH2*), for all tested conditions. Therefore, we also checked protein expression levels of nephrin and podocin to confirm their presence in SBAD2-derived podocytes grown on Geltrex using immunofluorescence staining (Fig. 7). Consistent with previously reported results, both nephrin and podocin protein expression was observed in iPSC-derived podocytes in this study (Rauch et al., 2018; Murphy et al., 2019). This inconsistency may be related to an issue with either the probes for these genes or could be a result of a difference in expression levels of mRNA and proteins related to these genes in these cells.

To gain a deeper understanding of the potential impact of alternative coatings on podocyte differentiation, two alternative coatings were selected and compared to Geltrex by full-genome TempO-Seq transcriptomics of one of the hiPSC lines (SBAD2). As no apparent differences had been observed among all five coatings in the previous characterizations, laminin-521 and the fibroblast-derived ECM were chosen due to their presence at high levels in the glomerular basement membrane *in vivo* (Lin et al., 2018) and the potential to more closely represent a biologically generated ECM, respectively.

The normalized transcriptomic read counts showed a high level of similarity among all the podocyte samples regardless of the coating and a clear distinction between them and the undifferentiated cells (Fig. 4A-B, 6B). While a relatively small number of genes was significantly impacted for the cells differentiated on both laminin-521 and fibroblast-ECM when compared to those differentiated on Geltrex (laminin-521 vs GT: 183 genes, fibroblast-ECM vs GT: 303 genes), several ECM-related genes were in the top 50 upregulated genes for both coatings. ITGA11, an integrin subunit and known component of podocyte ECM *in vivo* (Hammad et al., 2020), and HTRA1, a serine protease involved in ECM reorganization (Vierkotten et al., 2011) and in a web of proteases that direct the podocyte response to chemical, mechanical, and metabolic cues (Rinschen et al., 2018), were upregulated for both coatings. In addition, the podocytes differentiated on the fibroblast-ECM showed upregulation of VCAN (versican), an important ECM proteoglycan (Wight et al., 2020) that is produced by podocytes and contributes to the glomerular basement membrane (Björnson Granqvist et al., 2006).

In addition to comparing various alternative coatings for podocyte differentiation, we also improved the previously published protocol described in Rauch et al. (2018): (1) The glucose concentration of the medium used for podocyte differentiation and maintenance was reduced to 5 mM and (2) the seeding density at the start of differentiation was adjusted slightly, yielding more differentiated cells. Previous protocols described by us and others (Rauch et al., 2018; Song et al., 2012; Musah et al., 2018) used a relatively high concentration of glucose, i.e., 15-20 mM. Culturing podocytes in high glucose conditions (20 mM) has been shown to cause alterations of the expression of master regulators of oxidative metabolism and metabolic activity with patterns similar to those observed in patients with diabetic nephropathy compared to cells grown at a more physiological glucose concentration (5 mM) (Imasawa et al., 2017). The full genome TempO-Seq transcriptomics comparison between the originally and the currently described protocols appeared to be highly similar (Fig. S5[1]), and only 447 genes were differentially expressed between both protocols. Of these, no notable podocyte-specific, glomerular basement membrane-related genes or genes involved in glucose transport or metabolism were shown to be differentially expressed. Antibody staining for podocyte-specific proteins was comparable between the current protocol (Fig. 7) and the previously reported method (Rauch et al., 2018). While both glucose conditions seem to produce high-quality hiPSC-derived podocytes, the more physiological condition may be preferred, in particular when culturing podocyte-like cells in co-cultures or organ-on-chip devices that require a common medium for all cell types present. In summary, this updated protocol was able to produce podocyte-like cells of similar quality, but in greater numbers, using more physiological conditions.

4.4 Further optimization of fibroblast-ECM coating

The recombinant protein coatings tested in this study consist of single proteins, whereas Matrigel is a mixture of several ECM proteins, with the main components being laminin, entactin, and

collagen IV (Hughes et al., 2010). The question arose whether different single ECM proteins are sufficient or whether a combination of ECM proteins, as found *in vivo*, is superior for hiPSC maintenance and differentiation. It is a major challenge to recreate the *in vivo* ECM composition, as this is highly tissue-specific (Padhi and Nain, 2020) and often limited information is available on the ratio of proteins present. In the present study we could show that both single proteins (either truncated vitronectin or laminin-511/-521) as well as fibroblast-ECM consisting of potentially multiple proteins worked equally well for iPSC maintenance and differentiations into renal podocytes.

We also differentiated SBAD2 iPSCs into PTL using the different coatings as well as ECM generated from the proximal tubular cell RPTEC/TERT1 to compare the different coatings for differentiation into another cell type. While both ECM-coatings lead to similar morphology and staining patterns with the proximal tubular marker megalin and the tight junction marker ZO3 compared to Geltrex, the single-protein coatings did not deliver comparable results. This indicates that for some of the differentiation protocols ECM derived from human cell culture may have advantages over single recombinant human proteins. However, in addition to the successful differentiation of hiPSCs into renal podocyte-like cells in this study, many other successful differentiation protocols into other cell types have been reported on single human ECM proteins, including neurons on laminin-521 (Hyvärinen et al., 2019), hepatic cells on laminin-511 (Kanninen et al., 2016) and vitronectin (Nagaoka et al., 2015), and cardiomyocytes on laminin-521 (Burridge et al., 2014).

One major limitation of our study is that the ECM composition of dermal fibroblasts was not determined due to the challenge of measuring highly insoluble protein mixtures (Hughes et al., 2010). Therefore, we cannot comment on possible batch-to-batch variations although no overt variations were noticeable.

Another current limitation in the production of fibroblast-ECM using fHDF/TERT166 cells is their dependence on fetal bovine serum (FBS) in the culture medium. We acknowledge that serum-free culture is desirable and have started optimization of culture conditions. fHDF/TERT166 were originally cultured in medium containing 10% FBS when obtained from Evercyte GmbH; however, for both harvesting the ECM and routine culture of fibroblasts, we could lower this amount to 5% FBS with only a minor decrease in growth rate and without any compromise in the expression of the dermal fibroblast marker HSP47 (Fig. 1). A further reduction of FBS in the culture medium appears to be more challenging and could not be achieved within the time frame of this project. Nevertheless, work on reducing the culture media to 0% FBS was carried out in parallel, and preliminary results using a chemically-defined serum-free medium look promising. The adaptation procedure and full composition of this medium is described in the supplementary material1. Although this is still work in progress, it gives a very optimistic outlook that neonatal human fibroblasts can be successfully adapted to culture without FBS.

4.5 Cost comparison of alternative coatings

As described above, costs for recombinant coatings are unfortunately often higher than those for Matrigel. We calculated the cost for all commercial coatings based on prices from companies at the time of purchase. Note that these prices may differ between suppliers or may have changed since our assessment. The cost of coating one well of a 6-well plate varied substantially, with Geltrex being the cheapest at 0.24€ per well, followed by truncated vitronectin (produced in *E. coli*) at 0.49€ per well. Laminin-511 (produced under animal-origin free (AOF) conditions) and laminin-521 (produced xeno-free) more expensive at 1.74€ and 2.74€ per well, respectively. To estimate the cost for the in-house production of fibroblast-ECM and RPTEC/TERT1-ECM, we calculated the price of the main components of the culture medium in the volume necessary for three feeding cycles, which represents the culture time required before harvesting ECM. The price for coating one well with the medium used in this study was approximately 0.45€ and 0.39€ for fibroblast and RPTEC/TERT1-derived ECM, respectively. If, in future studies, the fibroblast medium can be adjusted to serum-free conditions (changing the medium components to AOF), this price would increase by 0.04€ to 0.49€. The RPTEC/TERT1 culture medium is already FBS-free.

This indicates that producing your own ECM using human cell lines can be a cost-effective alternative. Nevertheless, the amount of work required for culture of fibroblasts (or other types) needs to be considered, making these methods attractive to laboratories that culture these cell lines routinely for other applications.

4.6 Conclusions and recommendations

Here we performed an in-depth characterization, including full genome transcriptomics and whole genome shallow DNA sequencing, to compare commercially available human recombinant ECM protein coatings with the animal-derived Matrigel® (aka Geltrex™) for (1) long-term hiPSC maintenance culture and (2) hiPSC differentiation into renal podocyte-like cells. All the tested coatings, namely truncated vitronectin, laminin-511, and laminin-521 performed as well as Matrigel and can be recommended for both applications. Only very minor differences were found among different coatings, and no apparent compromises on pluripotency, karyotype stability or differentiation into EBs or podocyte-like cells were observed. In addition to avoiding working with animal-derived material, reported batch-to-batch variations of Matrigel could be avoided by switching to alternative coatings. Furthermore, we tested ECM harvested from human neonatal dermal fibroblasts for both hiPSC maintenance and differentiation into podocyte-like cells as a low-cost alternative to recombinant protein coatings. ECM that had been produced by decellularization was also highly comparable to all commercially available coatings for both applications. While these methods may still be prone to unidentified batch to batch variation, it may also be superior as a coating for more challenging differentiation protocols that may depend on the presence of several ECM proteins.

References

Albalushi, H., Kurek, M., Karlsson, L. et al. (2018). Laminin 521 stabilizes the pluripotency expression pattern of human

embryonic stem cells initially derived on feeder cells. *Stem Cells Int 2018*, 7127042. doi:10.1155/2018/7127042

Björnson Granqvist, A., Ebefors, K., Saleem, M. A. et al. (2006). Podocyte proteoglycan synthesis is involved in the development of nephrotic syndrome. *Am J Physiol Renal Physiol 291*, F722-F730. doi:10.1152/ajprenal.00433.2005

Braam, S. R., Zeinstra, L., Litjens, S. et al. (2008). Recombinant vitronectin is a functionally defined substrate that supports human embryonic stem cell self-renewal via alphavbeta5 integrin. *Stem Cells 26*, 2257-2265. doi:10.1634/stemcells.2008-0291

Burgeson, R. E., Chiquet, M., Deutzmann, R. et al. (1994). A new nomenclature for the laminins. *Matrix Biol 14*, 209-211. doi:10.1016/0945-053x(94)90184-8

Burridge, P. W., Matsa, E., Shukla, P. et al. (2014). Chemically defined generation of human cardiomyocytes. *Nat Methods 11*, 855-860. doi:10.1038/nmeth.2999

Chandrasekaran, V., Carta, G., da Costa Pereira, D. et al. (2021). Generation and characterization of iPSC-derived renal proximal tubule-like cells with extended stability. *Sci Rep 11*, 11575. doi:10.1038/s41598-021-89550-4

Chen, G., Gulbranson, D. R., Hou, Z. et al. (2011). Chemically defined conditions for human iPSC derivation and culture. *Nat Methods 8*, 424-429. doi:10.1038/nmeth.1593

Chichagova, V., Sanchez-Vera, I., Armstrong, L. et al. (2016). Generation of human induced pluripotent stem cells using RNA-based Sendai virus system and pluripotency validation of the resulting cell population. *Methods Mol Biol 1353*, 285-307. doi:10.1007/7651_2015_205

Fergus, J., Quintanilla, R. and Lakshmipathy, U. (2016). Characterizing pluripotent stem cells using the TaqMan® hPSC scorecard™ panel. *Methods Mol Biol 1307*, 25-37. doi:10.1007/7651_2014_109

Frantz, C., Stewart, K. M. and Weaver, V. M. (2010). The extracellular matrix at a glance. *J Cell Sci 123*, 4195-4200. doi:10.1242/jcs.023820

Garitaonandia, I., Amir, H., Boscolo, F. S. et al. (2015). Increased risk of genetic and epigenetic instability in human embryonic stem cells associated with specific culture conditions. *PLoS One 10*, e0118307. doi:10.1371/journal.pone.0118307

Hammad, S. M., Twal, W. O., Arif, E. et al. (2020). Transcriptomics reveal altered metabolic and signaling pathways in podocytes exposed to C16 ceramide-enriched lipoproteins. *Genes (Basel) 11*, 178. doi:10.3390/genes11020178

Hayman, E. G., Pierschbacher, M. D., Öhgren, Y. et al. (1983). Serum spreading factor (vitronectin) is present at the cell surface and in tissues. *Proc Natl Acad Sci U S A 80*, 4003-4007. doi:10.1073/pnas.80.13.4003

Hey, C. A. B., Saltõkova, K. B., Bisgaard, H. C. et al. (2018). Comparison of two different culture conditions for derivation of early hiPSC. *Cell Biol Int 42*, 1467-1473. doi:10.1002/cbin.10966

Holmes, R. (1967). Preparation from human serum of an alpha-one protein which induces the immediate growth of unadapted cells in vitro. *J Cell Biol 32*, 297-308. doi:10.1083/jcb.32.2.297

Hughes, C. S., Postovit, L. M. and Lajoie, G. A. (2010). Matrigel: A complex protein mixture required for optimal growth of cell culture. *Proteomics 10*, 1886-1890. doi:10.1002/pmic.200900758

Hyslop, L., Stojkovic, M., Armstrong, L. et al. (2005). Downregulation of NANOG induces differentiation of human embryonic stem cells to extraembryonic lineages. *Stem Cells 23*, 1035-1043. doi:10.1634/stemcells.2005-0080

Hyvärinen, T., Hyysalo, A., Kapucu, F. E. et al. (2019). Functional characterization of human pluripotent stem cell-derived cortical networks differentiated on laminin-521 substrate: Comparison to rat cortical cultures. *Sci Rep 9*, 17125. doi:10.1038/s41598-019-53647-8

Imasawa, T., Obre, E., Bellance, N. et al. (2017). High glucose repatterns human podocyte energy metabolism during differentiation and diabetic nephropathy. *FASEB J 31*, 294-307. doi:10.1096/fj.201600293r

Inoue, H., Nagata, N., Kurokawa, H. et al. (2014). IPS cells: A game changer for future medicine. *EMBO J 33*, 409-417. doi:10.1002/embj.201387098

Jacobs, K., Zambelli, F., Mertzanidou, A. et al. (2016). Higher-density culture in human embryonic stem cells results in DNA damage and genome instability. *Stem Cell Rep 6*, 330-341. doi:10.1016/j.stemcr.2016.01.015

Kang, X., Yu, Q., Huang, Y. et al. (2015). Effects of integrating and non-integrating reprogramming methods on copy number variation and genomic stability of human induced pluripotent stem cells. *PLoS One 10*, e0131128. doi:10.1371/journal.pone.0131128

Kanninen, L. K., Harjumäki, R., Peltoniemi, P. et al. (2016). Laminin-511 and laminin-521-based matrices for efficient hepatic specification of human pluripotent stem cells. *Biomaterials 103*, 86-100. doi:10.1016/j.biomaterials.2016.06.054

Khan, A. (2020). QDNAseq.hg38: QDNAseq bin annotation for the human genome build hg38. doi:10.5281/ZENODO.4274556

Kibbey, M. C. (1994). Maintenance of the EHS sarcoma and Matrigel preparation. *J Tissue Cult Methods 16*, 227-230. doi:10.1007/BF01540656

Kilpinen, H., Goncalves, A., Leha, A. et al. (2017). Common genetic variation drives molecular heterogeneity in human iPSCs. *Nature 546*, 370-375. doi:10.1038/nature22403

Lake, B. B., Chen, S., Hoshi, M. et al. (2019). A single-nucleus RNA-sequencing pipeline to decipher the molecular anatomy and pathophysiology of human kidneys. *Nat Commun 10*, 2832. doi:10.1038/s41467-019-10861-2

Lam, M. T. and Longaker, M. T. (2012). Comparison of several attachment methods for human iPS, embryonic and adipose-derived stem cells for tissue engineering. *J Tissue Eng Regen Med 6, Suppl 3*, s80-s86. doi:10.1002/term.1499

Li, H. (2013). Aligning sequence reads, clone sequences and assembly contigs with BWA-MEM. https://arxiv.org/abs/1303.3997v2 (accessed 16.12.2021)

Limonciel, A., Ates, G., Carta, G. et al. (2018). Comparison of baseline and chemical-induced transcriptomic responses in HepaRG and RPTEC/TERT1 cells using TempO-Seq. *Arch Toxicol 92*, 2517-2531. doi:10.1007/s00204-018-2256-2

Lin, M.-H., Miller, J. B., Kikkawa, Y. et al. (2018). Laminin-521 protein therapy for glomerular basement membrane and podocyte abnormalities in a model of Pierson syndrome. *J Am Soc Nephrol 29*, 1426-1436. doi:10.1681/ASN.2017060690

Liu, P., Kaplan, A., Yuan, B. et al. (2014). Passage number is a major contributor to genomic structural variations in mouse iPSCs. *Stem Cells 32*, 2657-2667. doi:10.1002/stem.1779

Love, M. I., Huber, W. and Anders, S. (2014). Moderated estimation of fold change and dispersion for RNA-seq data with DESeq2. *Genome Biol 15*, 550. doi:10.1186/s13059-014-0550-8

Lu, H. F., Chai, C., Lim, T. C. et al. (2014). A defined xeno-free and feeder-free culture system for the derivation, expansion and direct differentiation of transgene-free patient-specific induced pluripotent stem cells. *Biomaterials 35*, 2816-2826. doi:10.1016/j.biomaterials.2013.12.050

Lu, J., Baccei, A., Lummertz da Rocha, E. et al. (2018). Single-cell RNA sequencing reveals metallothionein heterogeneity during hESC differentiation to definitive endoderm. *Stem Cell Res 28*, 48-55. doi:10.1016/j.scr.2018.01.015

Lu, Y., Ye, Y., Bao, W. et al. (2017). Genome-wide identification of genes essential for podocyte cytoskeletons based on single-cell RNA sequencing. *Kidney Int 92*, 1119-1129. doi:10.1016/j.kint.2017.04.022

Meredith, J. E., Winitz, S., Lewis, J. M. A. et al. (1996). The regulation of growth and intracellular signaling by integrins. *Endocr Rev 17*, 207-220. doi:10.1210/edrv-17-3-207

Morrison, M., Klein, C., Clemann, N. et al. (2015). StemBANCC: Governing access to material and data in a large stem cell research consortium. *Stem Cell Rev 5*, 681-687. doi:10.1007/s12015-015-9599-3

Murphy, C., Feifel, E., Jennings, P. et al. (2019). A protocol for one-step differentiation of human induced pluripotent stem cells into mature podocytes. *Methods Mol Biol 1994*, 93-99. doi:10.1007/978-1-4939-9477-9_8

Musah, S., Dimitrakakis, N., Camacho, D. M. et al. (2018). Directed differentiation of human induced pluripotent stem cells into mature kidney podocytes and establishment of a glomerulus chip. *Nat Protoc 13*, 1662-1685. doi:10.1038/s41596-018-0007-8

Nagaoka, M., Kobayashi, M., Kawai, C. et al. (2015). Design of a vitronectin-based recombinant protein as a defined substrate for differentiation of human pluripotent stem cells into hepatocyte-like cells. *PLoS One 10*, e0136350. doi:10.1371/journal.pone.0136350

Nagasaka, R., Matsumoto, M., Okada, M. et al. (2017). Visualization of morphological categories of colonies for monitoring of effect on induced pluripotent stem cell culture status. *Regen Ther 6*, 41-51. doi:10.1016/j.reth.2016.12.003

Pace, J. A., Bronstein, R., Guo, Y. et al. (2021). Podocyte-specific KLF4 is required to maintain parietal epithelial cell quiescence in the kidney. *Sci Adv 7*, eabg6600. doi:10.1126/sciadv.abg6600

Padhi, A. and Nain, A. S. (2020). ECM in differentiation: A review of matrix structure, composition and mechanical properties. *Ann Biomed Eng 48*, 1071-1089. doi:10.1007/s10439-019-02337-7

Pan, G. and Thomson, J. A. (2007). Nanog and transcriptional networks in embryonic stem cell pluripotency. *Cell Res 17*, 42-49. doi:10.1038/sj.cr.7310125

Quinlan, A. R. and Hall, I. M. (2010). BEDTools: A flexible suite of utilities for comparing genomic features. *Bioinformatics 26*, 841-842. doi:10.1093/bioinformatics/btq033

Rauch, C., Feifel, E., Kern, G. et al. (2018). Differentiation of human iPSCs into functional podocytes. *PLoS One 13*, e0203869. doi:10.1371/journal.pone.0203869

Refaeli, I., Hughes, M. R., Wong, A. K.-W. et al. (2020). Distinct functional requirements for podocalyxin in immature and mature podocytes reveal mechanisms of human kidney disease. *Sci Rep 10*, 9419. doi:10.1038/s41598-020-64907-3

Rinschen, M. M., Huesgen, P. F. and Koch, R. E. (2018). The podocyte protease web: Uncovering the gatekeepers of glomerular disease. *Am J Physiol Renal Physiol 315*, F1812-F1816. doi:10.1152/ajprenal.00380.2018

Rodin, S., Domogatskaya, A., Ström, S. et al. (2010). Long-term self-renewal of human pluripotent stem cells on human recombinant laminin-511. *Nat Biotechnol 28*, 611-615. doi:10.1038/nbt.1620

Rodin, S., Antonsson, L., Niaudet, C. et al. (2014). Clonal culturing of human embryonic stem cells on laminin-521/E-cadherin matrix in defined and xeno-free environment. *Nat Commun 5*, 3195. doi:10.1038/ncomms4195

Rowland, T. J., Miller, L. M., Blaschke, A. J. et al. (2010). Roles of integrins in human induced pluripotent stem cell growth on Matrigel and vitronectin. *Stem Cells Dev 19*, 1231-1240. doi:10.1089/scd.2009.0328

Scheinin, I., Sie, D., Bengtsson, H. et al. (2014). DNA copy number analysis of fresh and formalin-fixed specimens by shallow whole-genome sequencing with identification and exclusion of problematic regions in the genome assembly. *Genome Res 24*, 2022-2032. doi:10.1101/gr.175141.114

Singh, P., Chandrasekaran, V., Hardy, B. et al. (2021). Temporal transcriptomic alterations of cadmium exposed human iPSC-derived renal proximal tubule-like cells. *Toxicol In Vitro 76*, 105229. doi:10.1016/J.TIV.2021.105229

Slamecka, J., McClellan, S., Wilk, A. et al. (2018). Induced pluripotent stem cells derived from human amnion in chemically defined conditions. *Cell Cycle 17*, 330-347. doi:10.1080/15384101.2017.1403690

Song, B., Smink, A. M., Jones, C. V. et al. (2012). The directed differentiation of human iPS cells into kidney podocytes. *PLoS One 7*, e46453. doi:10.1371/journal.pone.0046453

Suter-Dick, L., Alves, P. M., Blaauboer, B. J. et al. (2015). Stem cell-derived systems in toxicology assessment. *Stem Cells Dev 24*, 1284-1296. doi:10.1089/scd.2014.0540

Suzuki, S., Oldberg, A., Hayman, E. G. et al. (1985). Complete amino acid sequence of human vitronectin deduced from cDNA. Similarity of cell attachment sites in vitronectin and fibronectin. *EMBO J 4*, 2519-2524. doi:10.1002/j.1460-2075.1985.tb03965.x

Takahashi, K. and Yamanaka, S. (2006). Induction of pluripotent stem cells from mouse embryonic and adult fibroblast cultures by defined factors. *Cell 126*, 663-676. doi:10.1016/j.cell.2006.07.024

Theocharis, A. D., Skandalis, S. S., Gialeli, C. et al. (2016).

Extracellular matrix structure. *Adv Drug Deliv Rev 97*, 4-27. doi:10.1016/j.addr.2015.11.001

Tsankov, A. M., Akopian, V., Pop, R. et al. (2015). A qPCR ScoreCard quantifies the differentiation potential of human pluripotent stem cells. *Nat Biotechnol 33*, 1182-1192. doi:10.1038/nbt.3387

Vierkotten, S., Muether, P. S. and Fauser, S. (2011). Overexpression of HTRA1 leads to ultrastructural changes in the elastic layer of Bruch's membrane via cleavage of extracellular matrix components. *PLoS One 6*, e22959. doi:10.1371/journal.pone.0022959

van de Wiel, M. A., Kim, K. I., Vosse, S. J. et al. (2007). CGHcall: Calling aberrations for array CGH tumor profiles. *Bioinformatics 23*, 892-894. doi:10.1093/bioinformatics/btm030

Wieser, M., Stadler, G., Jennings, P. et al. (2008). hTERT alone immortalizes epithelial cells of renal proximal tubules without changing their functional characteristics. *Am J Physiol Renal Physiol 295*, F1365-F1375. doi:10.1152/ajprenal.90405.2008

Wight, T. N., Kang, I., Evanko, S. P. et al. (2020). Versican – A critical extracellular matrix regulator of immunity and inflammation. *Front Immunol 11*, 512. doi:10.3389/fimmu.2020.00512

Wilmes, A., Rauch, C., Carta, G. et al. (2017). Towards optimisation of induced pluripotent cell culture: Extracellular acidification results in growth arrest of iPSC prior to nutrient exhaustion. *Toxicol In Vitro 45*, 445-454. doi:10.1016/j.tiv.2017.07.023

Wolford, J. L., Chishti, Y., Jin, Q. et al. (2010). Loss of pluripotency in human embryonic stem cells directly correlates with an increase in nuclear zinc. *PLoS One 5*, e12308. doi:10.1371/journal.pone.0012308

Young, J. C., Major, A. T., Miyamoto, Y. et al. (2011). Distinct effects of importin α2 and α4 on Oct3/4 localization and expression in mouse embryonic stem cells. *FASEB J 25*, 3958-3965. doi:10.1096/fj.10-176941

Zhang, P., Andrianakos, R., Yang, Y. et al. (2010). Kruppel-like factor 4 (Klf4) prevents embryonic stem (ES) cell differentiation by regulating nanog gene expression. *J Biol Chem 285*, 9180-9189. doi:10.1074/jbc.M109.077958

Conflict of interest

The authors declare no conflict of interest.

Data availability

The raw read counts of the TempO-Seq transcriptomics are included in the supplementary material[1]. All other research data described in the manuscript is available from the corresponding author upon reasonable request.

Acknowledgements

This research was funded by a grant from the *Stiftung zur Förderung der Erforschung von Ersatz- und Ergänzungsmethoden zur Einschränkung von Tierversuchen* (Stiftung SET) (to AW).